A Review of Packed Bed Reactor and Gradient-less Recycle Reactor for Determination of Intrinsic Reaction Kinetics

Khunnawat Ountaksinkul[1,2]**, Sirada Sripinun**[1]**, Panut Bumphenkiattikul**[3,4]**,
Arthit Vongachariya**[3,4]**, Piyasan Praserthdam**[1]**, and Suttichai Assabumrungrat**[1,2,*]

[1] Center of Excellence on Catalysis and Catalytic Reaction Engineering, Department of Chemical Engineering, Faculty of Engineering, Chulalongkorn University, Bangkok 10330, Thailand
[2] Bio-Circular-Green-economy Technology & Engineering Center (BCGeTEC), Faculty of Engineering, Chulalongkorn University, Bangkok 10330, Thailand
[3] Advanced Process Modeling, Digital Manufacturing Technology Group, Olefins and Operations Technology, Chemicals Business, SCG, Thailand
[4] The Thai Institute of Chemical Engineering and Applied Chemistry, Thailand
*E-mail: Suttichai.a@chula.ac.th (Corresponding author)

Abstract. Intrinsic reaction kinetics is an essential information in catalytic reaction engineering. This paper reviews the two laboratory reactors, i.e., the packed-bed reactor and gradient-less recycle reactor commonly employed for determining the intrinsic reaction kinetics of heterogeneous catalysts. Although both reactors have been well-known for kinetic studies for a long time, there are still efforts to address some essential issues and to further develop the reactors. For example, a new design of the gradient-less recycle reactor was developed to broaden the operating window for intrinsic kinetic studies at low pressure. Furthermore, the intrinsic kinetic modeling in the gradient-less recycle reactor and packed-bed reactor, including the effects of mass transfer and axial dispersion, was also investigated. This review article provides in detail the types of both reactors, the development of both packed-bed reactor and gradient-less recycle reactor, intrinsic kinetic modeling, and the methods for determining heat- and mass- transfer limitations. All of these point out the suitable methods for determining intrinsic kinetics and perspectives for future works.

Keywords: Gradient-less recycle reactor, packed bed reactor, intrinsic kinetics, high-throughput experimentation, mass transfer, heat transfer.

1. Introduction

In chemical industries, reaction kinetics is a key to successful development of new chemical processes as well as improvement of existing catalytic processes. The process development starts from conceptualizing the idea for a new process or catalyst, catalyst preparation and screening, creating reaction networks, reaction kinetic studies, stability test, and scaling up to pilot and commercial-scale reactors [1]. During the development, knowledge involving catalytic reaction engineering, as shown in Fig. 1, has been studied to understand the chemical reactions taking place in the reactor and achieve intrinsic kinetics from the experiments [1-3]. This review focuses on the methods for the kinetic experiments in the laboratory catalytic reactors and kinetic modeling. Kinetic modeling is the transformation of the behavior of a chemical process into mathematical models applied with several simulations to improve and develop the chemical processes [2]. Figuratively, the kinetic model is a bridge between laboratory studies and commercial chemical processes. Basically, the kinetic modeling includes three steps: [4]

1. Obtaining experimental kinetic data for several conditions of composition, temperature, and pressure
2. Providing a suitable selection of rate expression and reaction network (e.g., Power-law model, and LHHW model)
3. Finding the proper consideration of the unknown kinetic parameters in the rate expression

Several types of reactors can be applied to determine this worthwhile information above, and it is crucial to choose a reactor to acquire the experimental kinetic data suitably. Typically, the standard for selecting a laboratory reactor for catalyst testing is considerably different from the criteria for selecting the industrial reactor [1]. Scaling down from the commercial to laboratory scale is satisfactory due to lower investment and operating costs, less utility requirement, lower waste formation, and higher work safety (lower opportunities for toxic emissions, fire, and explosion) than the industrial reactor [1]. Therefore, various laboratory reactors have been investigated to determine reaction kinetics in the industrial reactor for a long time.

In general, performing a reaction in ideal reactor types, i.e., plug flow reactor (PFR) and continuous stirred-tank reactor (CSTR), has been well-known as a common method for kinetic studies. Recently, there are other techniques such as steady-state isotopic transient kinetic analysis (SSITKA), In situ/Operando method, and temporal analysis of products (TAP) method developed to study reaction micro-kinetics intensely; however, both plug flow reactor (PFR) and continuous stirred-tank reactor (CSTR) have still been widely used for the kinetic experiments due to their simple operating system and low investment cost [5-8]. Notably, the reliability of reaction kinetics is a key challenge of researchers [2]. Although fluid seems to be "plug flow" throughout the catalyst bed in the plug flow reactor, when considering the fluid flow around the catalyst particles, as shown in Fig. 2, the mixing dispersion can occur at the particle size level [1]. While for CSTR, the non-ideal flow characteristics such as channeling, stationary region or dead-zone, and back-mixing can be observed in this reactor [9, 10]. These phenomena certainly affect reactor performance and kinetic modeling.
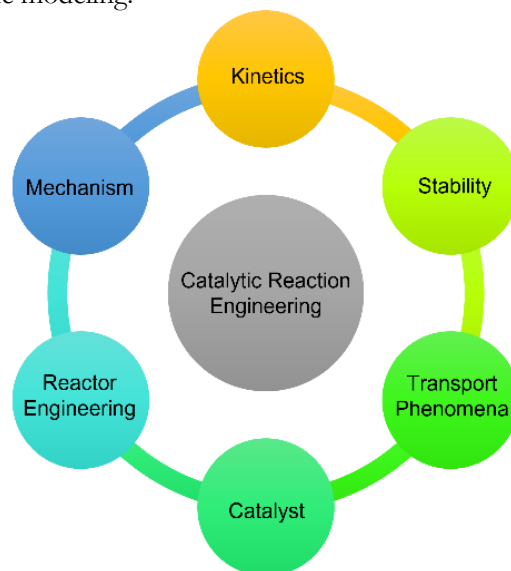

Fig. 1. Catalytic reaction engineering.

Moreover, the catalytic reaction process is also influenced by mass diffusion. As shown in Fig. 2, while reactants are slowly converted along the catalyst bed, it needs to diffuse from the bulk fluid to a stagnant layer around the catalyst particles. This phenomenon is called "external mass transfer" [11]. Subsequently, the reactants move into the pore structure of the catalyst particles to an active site where a chemical reaction occurs, as called "internal mass transfer" [12]. On the other hand, the products will diffuse oppositely. In many cases, heat energy can be produced or consumed, depending on the exothermic and endothermic processes of reactions. This results in a temperature gradient in the local area of the reactor. Therefore, the heat should be removed or supplied at a sufficient rate to maintain the desired temperature to avoid heat transfer limitation. The observed reaction rate is probably dominated by the mentioned mass- and heat-transfer limitations; therefore, the reaction kinetics can be classified into three categories: extrinsic kinetics, apparent kinetics, and intrinsic kinetics. Remarkably, the intrinsic kinetics represents only the chemical reaction on the catalyst surface compared to the others, which still include the effects of transport phenomena. In addition, it is well-known that the following conditions should be provided to obtain the intrinsic kinetics effectively [1]:

1. Very good contact between catalyst and reactants
2. Eliminated mass and heat transfer limitations both outside and inside the catalysts
3. Well-defined described reactor characteristics, residence time distribution, and isothermal condition (ideal system)
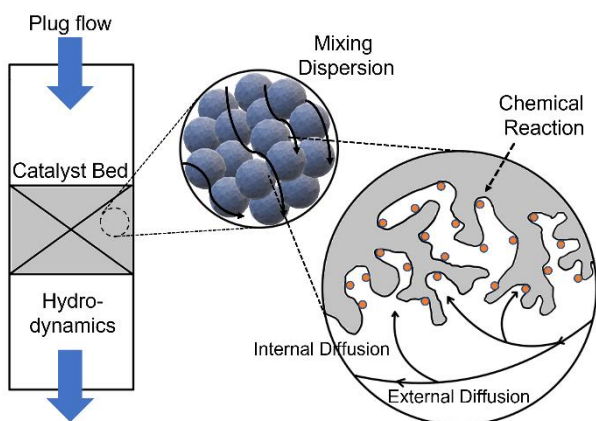
Fig. 2. Transport phenomena in a fixed bed reactor on the different diffusion levels (Adapted from [1]).

Over the past 30 years, several research teams have published reviews on reaction kinetics in various aspects. Perego and Peratello (1999) reviewed experimental methods and suitable reactors for evaluating kinetics of a catalytic process. Berger et al. (2001) reviewed various kinetic models and reaction kinetics in practice [2, 13]. Kapteijn and Moulijn (2008) reviewed reactor systems, types of laboratory reactors, design equations, and criteria for mass and heat transfers [1]. However, there are still advancements in the kinetic determination in several aspects such as development of new reactors/systems, and applications of computational tools for understanding phenomena in the reactors over the past decade. Therefore, additional information is provided in this review article.

In this work, various methods for investigating reaction kinetics, especially intrinsic kinetics and catalyst testing approach in steady-state laboratory catalytic reactors, were reviewed for a heterogeneous catalytic system. This system includes the solid phase of the catalyst and the gaseous and/or liquid phase of the substance. The different types of plug flow reactor (PFR) and continuous stirred-tank reactor (CSTR), as the well-known methods, were explained with the pros and cons of each method in an aspect of intrinsic kinetics determination. Furthermore, the current trends for catalyst testing were also described.

2. Laboratory Reactors for Kinetic Determination

Different reactor types have been explained in literatures [14-17]. They can be mainly divided into five categories depending on the reaction system investigated: gas-solid (GS), liquid-solid (LS), gas-liquid-solid (GLS), liquid-gas (LS), and liquid (L) systems [4]. The first three refer to solid (immobilized) catalysts, while the last two relate to homogeneous catalytic reactions, which are not included in this review. The existence of two reaction phases needs to be avoided as far as possible for the easiness of data interpretation and experimentation. In this review, several laboratory reactors for kinetic determination in the first three systems are described as follows.

According to J. M. Berty (1999), various experimental methods for kinetic measurement have been investigated in the last century [18]. They were continuously developed with the evolution of the chemical industries. In the 1940s, a tubular reactor was used as a common tool for kinetic studies by considering conversion versus residence time. Then, in the 1950s, the kinetic experiment in a differential reactor became a well-known method. Subsequently, in the 1960s, a Continuous Stirred Tank Reactor (CSTR) started to gain interest for kinetic studies [18]. Various types of CSTRs were established to investigate the heterogeneous catalytic reactions, including spinning basket CSTRs and many kinds of fixed bed reactors with the external or internal recycle pumps. In the 1990s, various transient experimental methods such as temporal analysis of products (TAP) reactor and steady-state isotopic transient kinetic analysis (SSITKA) technique for kinetic measurement have been developed to intensely investigate the sequences of reaction network and kinetic modeling [19, 20]. Furthermore, modern technologies such as high-throughput experimentation (HTE), microchannel reactors have been proposed for catalyst screening and kinetic studies as well.

Operation of catalytic reactors can be categorized into steady-state and unsteady state modes. Both plug flow reactor (PFR) and continuous stirred-tank reactor (CSTR) are classified as the steady-state mode. In contrast, the examples of transient mode are batch CSTR reactor, steady-state isotopic transient kinetic analysis (SSITKA), temporal analysis of products (TAP) reactor, and so on. The transient operation for kinetic studies is relatively uncommon because of some disadvantages for the catalyst testing approach. Catalyst deactivation is one of the problems for the batch reactor because it cannot be measured during batch experiments [21]. It is necessary to repeat the experiment to verify the effect of catalyst deactivation. In TAP reactors, the catalyst is tested under specific operating conditions, which absolutely differ from industrial conditions or steady-state operation [22-24]. Nevertheless, these unsteady-state operations were mainly used to obtain valuable information about reaction mechanisms and establish reaction networks [24]. Still, the steady-state isotope transient kinetic analysis (SSITKA) approach can offer both sequences of reaction mechanism and steady-state information [25-27].

In this review, we focus on steady-state laboratory catalytic reactors. These reactors can be categorized for kinetic studies by the two flow regimes; 1. Plug flow, and 2. Mixed flow. The plug flow behavior can be represented in the integral and differential packed bed reactor. In contrast, various types of CSTRs, gradient-less recycle reactor, and fluidized bed reactor were operated with the mixed flow regime. According to Perego and Peratello (1999), the different types of laboratory catalytic reactors were summarized in the schematic diagram as shown in Fig. 3 [13]. It is well-known that there is no best laboratory reactor for all types of reactions and catalysts. It depends

on the reaction system, severe or mild operating conditions, and other factors. In this section, each type of steady-state laboratory catalytic reactor was discussed for catalyst testing and determination of the kinetic parameters. According to Kapteijn and Moulijn (2008), a generalized comparison of frequently-used laboratory reactors was shown in their literature [1]. More information on plug flow reactor and gradient-less recycle reactor is described in the following sections.
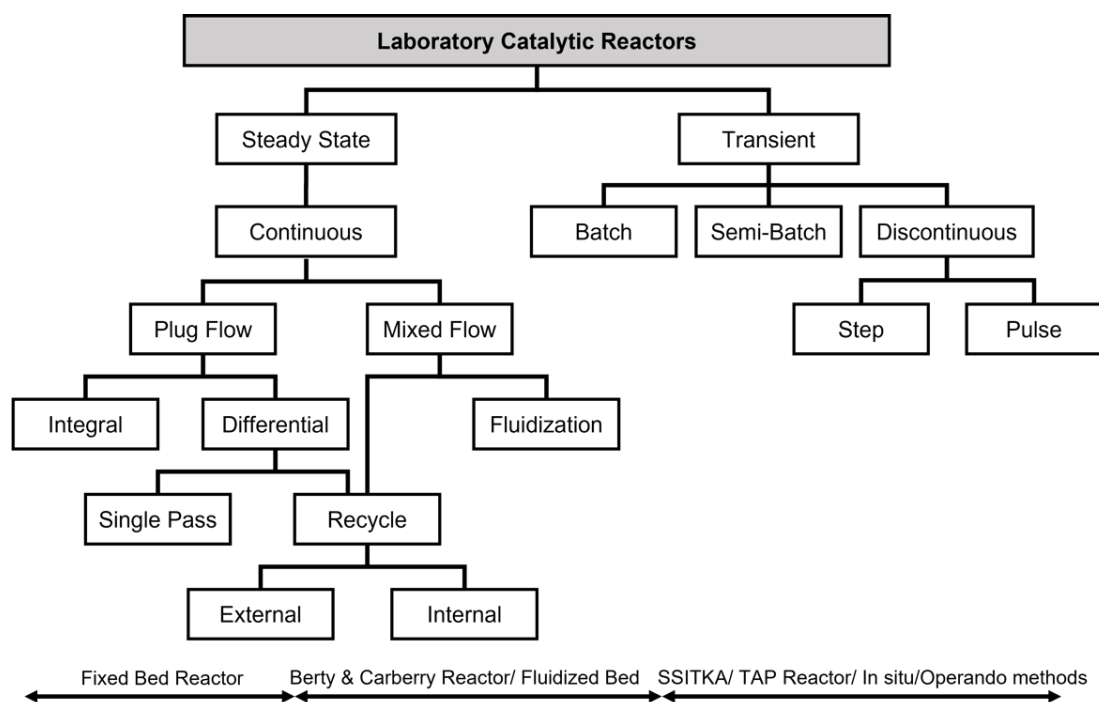

Fig. 3. Different types of laboratory catalytic reactors (Adapted from [13]).

2.1. Plug Flow Reactor

The simplest reactor type of laboratory reactor for catalyst testing of heterogeneous catalytic reactions is a fixed bed tubular reactor, as shown in Fig. 4(a). This fixed bed reactor can be used for both gas-solid and liquid-solid reactions. Generally, the catalyst is packed at the center of a tubular tube and plugged by quartz wool or wire mesh gauze on both sides. The reactor is usually set vertically to ensure that the catalyst is uniformly packed as far as possible. In many cases, inert balls or ceramic balls are used to disperse the reactant flow in the radial direction and avoid fluidization in up-flow configurations. Normally, the packed bed reactor is placed in a furnace and a thermocouple was installed to measure temperature in the catalyst bed. It should be concerned that the flow pattern of the packed bed reactor must not be disturbed by channeling along the thermocouple wall. The tubular tube for the fixed bed reactor can be made of glass, quartz, steel, or ceramic depending on severe or mild operating conditions. Glass can be applied for low pressure and temperature, whereas steel is used for high pressure [1]. For quartz and ceramic, they can be operated under high-temperature conditions.

There are different shapes of packed bed reactor such as straight pipe, U-shape, or concentric geometry, with the catalyst packed within the tube [28]. The suitable inner diameter (D) for packed bed reactor is about 4-6 mm to provide effective heat transfer inside the reactor [29].

Moreover, according to Perego and Peratello (1999), the plug flow regime can be achieved by the following conditions [13]:

- The inner diameter of the reactor (D) should be greater than that of catalyst particle (d_p) at least > 10 times [30].
- For gas-solid reactions, the catalyst bed length (L) must be larger than the diameter of the catalyst particle (d_p) at least 50 times ($L/d_p > 50$).
- For liquid-solid reactions, the catalyst bed length (L) should be much larger than the particle diameter (d_p) several hundred times, at the relatively low flow in laboratory reactors.

However, the axial dispersion, fluctuations due to different flow velocities, molecular and turbulent diffusion should be concerned for packed bed reactor [31]. For limitations of mass- and heat- transfers in packed bed reactor, the theoretical criteria and the different experimental methods were described in section 4.

Compared with the gradient-less recycle reactor, the packed bed reactor is significantly smaller. The volume of the gradient-less recycle reactor is usually greater than 100 cm³, whereas the amount of catalyst per volume of the gradient-less recycle reactor is smaller, about 2 to 3 times [1]. Because of this reason, it refers to the different physical residence times in both reactors.

2.1.1. Differential and integral packed bed reactors

In general, the packed bed reactor can be operated in two different forms: differential form (low conversion < 5%) and integral form (relatively high conversion), as shown in Fig. 4(b). Both types were carried out with different catalyst volumes and space velocities.
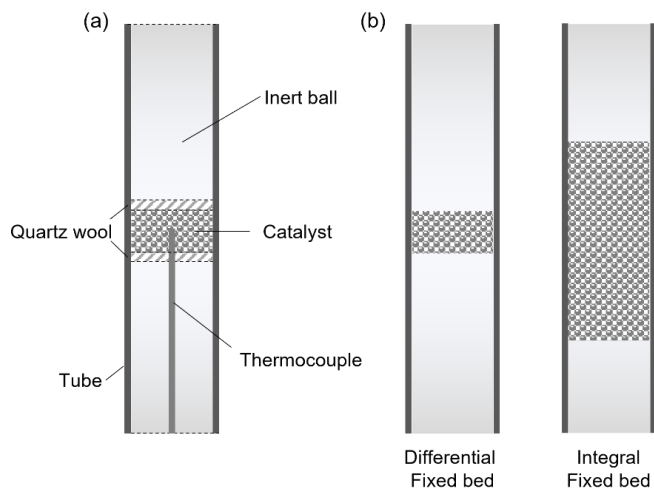

Fig. 4. (a) The components of fixed bed tubular reactor and (b) the common types of packed bed reactor.

Figure 5 shows the concentration profiles of both differential and integral packed bed reactors, as well as the gradient-less, recycle reactor. Theoretically, both differential and integral packed bed reactors have a concentration gradient inside the catalyst bed according to plug flow behavior. In contrast, the gradient-less recycle reactor cannot be observed due to the perfect mixing behavior. The reactant concentration in the differential reactor is higher than that in the integral reactor due to the lower amount of the catalyst resulting in low conversion. These exit concentrations relate to catalytic activity, thermodynamics, and the hydrodynamic regime of the reactor. Nowadays, the differential packed bed reactor is much more popular than the integral one due to smaller catalyst loading and better control of a temperature gradient [13]. In addition, the concentration profile in the gradient-less recycle reactor was described in section 2.2.

2.1.2. Development of plug flow reactor

Currently, both differential and integral packed bed reactors have been widely used as the common reactors for kinetic modeling and investigating catalytic activities. Nevertheless, the plug flow reactor has been continuously developed due to some mass- and heat- transfer restrictions as shown in section 4. Consequently, the compact system of the microchannel reactor began to be studied to improve the efficiency for mass- and heat-transfers. Due to the high surface-to-volume ratio of a microchannel reactor, it results in excellent mass- and heat-transfers as well as a higher conversion than other reactors [32]. Several applications and uses for the process

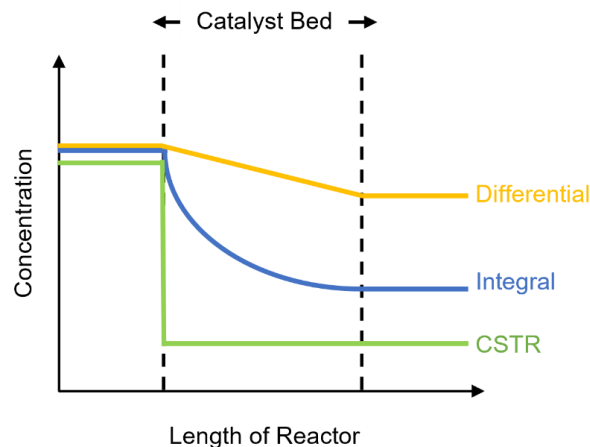development of the microchannel reactor were clearly reviewed in the literature [33-35].

Fig. 5. Comparison of reactant concentration profiles for the typical laboratory reactors for kinetic measurement.

For kinetic modeling in micro-scale, according to Peela and Kunzru (2011), the microchannel reactor was used for the kinetic study of ethanol steam reforming [36]. They found that the kinetic expression based on the Langmuir-Hinshelwood model could predict the experimental data satisfactorily. The ideal plug flow model was also applied in their research to represent the microchannel reactor [36]. Moreover, the mass- and heat-transfer limitations could be neglected in microchannel reactor. Additionally, the kinetic studies for ionic liquid synthesis of 1-butyl-3-methylimidazolium bromide, photocatalytic CO_2 reduction, direct synthesis of hydrogen peroxide, methanol steam reforming, and so on were investigated in the microchannel reactor as well [37-40].

In addition, a wall-coated microreactor was employed for kinetic studies. For example, the wall-coated microchannel reactor was used to study reaction kinetics of hydrogen peroxide synthesis [39]. Randomly packed structure of packed bed-microchannel reactor can lead to a high pressure drop and flow maldistribution. Besides, for synthesis of hydrogen peroxide, hot spots can be also formed due to improper dilution with inert material. Consequently, the use of the wall-coated microreactor can eliminate the temperature gradient presenting in micro packed-bed and also improve mass transfer rate [39].

Recently, high-throughput experimentation has been developed to test many catalysts in parallel operation. Each parallel acts as a single plug flow reactor. Therefore, this high-throughput experimentation is often used for catalyst screening. Figure 6 shows the historical trend for the number of research publications about the fixed bed reactor in an aspect of reaction kinetics as well as gradient-less recycle reactor and high-throughput experimentation based on the database of Scopus over 70 years. Although the packed bed reactor was first developed to investigate the reaction kinetics in the 1940s before using the gradient-less recycle reactor and others, it has been still widely studied due to the simplest experimental system, low costs, and simple interpretation of kinetic data. For gradient-less recycle reactor, it started to get attention for kinetic studies

since the 1960s; however, the number of research publications of this reactor is much lower than that of the packed bed reactor over the half-century. It may be due to the limitation of mixing characteristics under some operating conditions in the original gradient-less recycle reactor. This was additionally explained below. For both packed bed reactor and gradient-less recycle reactor, these conventional catalyst testing approaches involve the evaluation of a single or a few catalyst compositions under variation of operating conditions in a single reactor system. To solve this issue, further innovations have developed as so-call parallelization or "high-throughput experimentation (HTE)" and microchannel reactor.
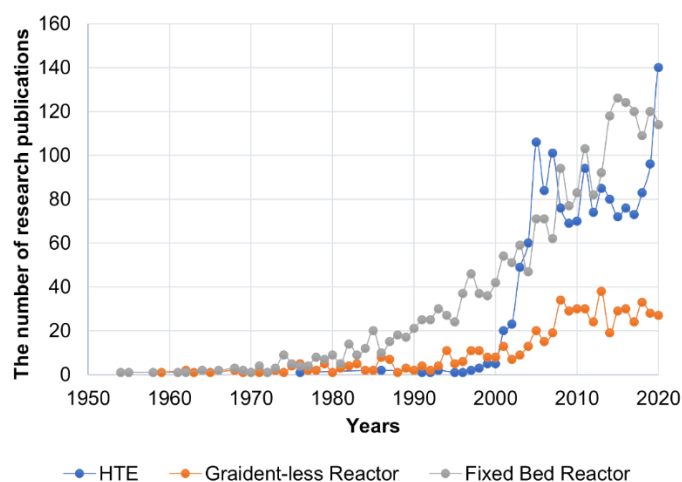

Fig. 6. The number of research publications about the kinetic studies in fixed bed reactor, gradient-less recycle reactor and high-throughput experimentation based on the database of Scopus (Accessed Aug 31, 2021).

The high-throughput experimentation can allow testing the catalysts in parallel operation with the robotic synthesis to screen for a new catalyst. As shown in Fig. 7, the number of research publications for HTE systems has considerably increased since the 2000s. Details of the design, implementation and verification for a catalyst testing system with the six microchannel reactors in parallel were published in the literature [41]. Several prototypes of these systems have been commercialized nowadays. High-throughput experimentation has been widely used in various research areas. According to the database of Scopus, as shown in Fig. 7, the high-throughput experimentation can be applied with the research in fields of Chemistry (19%), Biochemistry (14%), Chemical engineering (14%), Engineering (10%), and many more.

Besides the application for catalyst screening, high-throughput experimentation was used for kinetic studies [42, 43]. The high-throughput experimentation offers opportunities for accurate and rapid data acquisition for several chemical reactions such as hydrocracking, isomerization, syngas conversion, and so on [42]. In general, one reactor acts as the reference packed with inert particles, whereas the different amounts of the catalyst fill the other reactors in parallel to investigate the variation of

the contact time (W/F) [1]. Moreover, the requirement of rapid catalyst testing devices with additional miniaturization is one of the key issues to improve performance of these parallel fixed bed reactor systems [44].
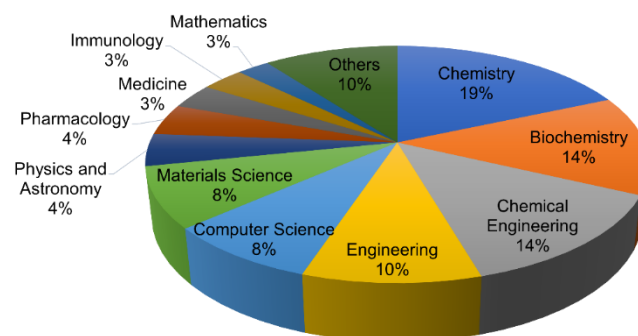

Fig. 7. (a) The research area for the high-throughput experimentation based on the database of Scopus (Accessed Aug 31, 2021).

Recently, the microchannel reactor with a very large number of parallel channels, which have a diameter from 10 to several hundred micrometers [1], has been developed. Because of very small dimensions, the microchannel reactors have a very high surface-to-volume ratio resulting in good heat and mass transfers inside this reactor [32]. Therefore, these microchannel reactors can be used for catalyst testing under the suitable condition of kinetic controls. Mies et al. (2007) proposed a high-throughput microreactor (HTMR) with the eight different catalyst coatings with a turnover frequency of $0.1 - 10$ s^{-1} at a flow rate from 50 to 100 cm^3 min^{-1} [45, 46]. These operating windows allow the coated catalysts to be tested in the differential reactor mode. It greatly simplifies the interpretation of kinetic data. Moreover, the advantage of catalyst coatings is low-pressure drop in contrast to the microchannel reactors filled with the catalyst powder [1, 47, 48].

However, there are some problems with catalyst deactivation and reproducibility. According to Ehm et al. (2020), high-throughput experimentation was investigated in olefin polymerization [43]. They found that controlling fast reactions in HTMRs at the very small catalyst loading was difficult due to catalyst species being easily deactivated by the impurities. It led to poor reproducibility in some conditions for the HTE microchannel reactors.

According to Hazemann et al. (2020), they studied the high-throughput Fischer-Tropsch experimentation [42]. They found that variation of catalyst amounts in the HTE system is appropriate only for the case of easily reducible catalysts. The catalysts in all parallel reactors should be uniform or provide the same extent of the reduction. In some chemical reactions such as Fischer-Tropsch synthesis, the less reducible cobalt catalysts in their work were reduced nonuniformly. These led to incoherent kinetic data. Moreover, the problem of catalyst deactivation and the accumulation of wax products were also found in HTE for Fischer-Tropsch synthesis. Using

successive short tests can avoid the catalyst deactivation; however, the catalyst deactivation can significantly affect at high conversion level.

2.2. Gradient-less Recycle Reactor

In this review, the reactor types of continuous stirred-tank reactor (CSTR) include both gradient-less internal and external recycle reactors. In gradient-less recycle reactor, both reactant and product are recirculated internally or externally at a sufficiently high mixing degree to confirm that the reactant and product concentrations are certainly constant in every part of the reactor [30]. In most cases, this proceeds with the continuous process. There is steady reactant flow entering into the reactor and exit flow of the reaction mixture at another position relating to the bed. As shown in Fig. 8, the difference between the inlet and outlet flow rates of reactant in the catalyst bed is equivalent to the reaction rate. If the recirculation rate is sufficiently high compared with the reaction rate, the outlet concentrations of both reactant and product are the same throughout the reactor.
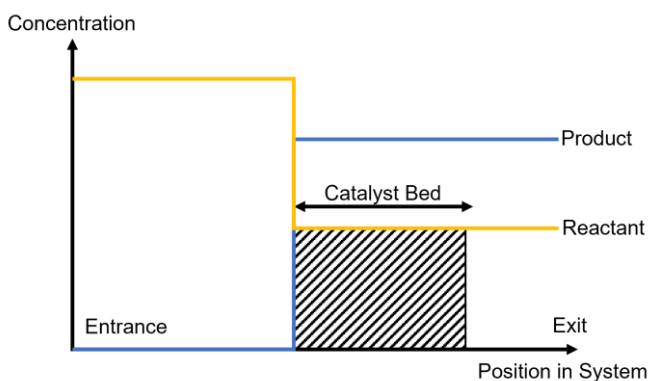

Fig. 8. Typical profiles through a gradient-less recycle reactor.

As shown in Fig. 8, the concentration of the reactant is constant until the first point before entering the catalyst bed. After that, the concentration of the reactant is immediately changed by the chemical reaction and keeps this concentration value until the exit. On the other hand, product concentration instantly increases after the reactant flow enters the catalyst bed. The advantage of the gradient-less recycle reactor over other reactor types is that the reaction rate can be directly estimated by the reactant flow rate and conversion. The mathematical model for kinetic modeling is much simpler than the other reactors. However, many factors probably affect a deviation from the ideal profile [30]. It is necessary to investigate the ideality of the gradient-less recycle reactor for kinetic studies. In general, the four types of gradient-less recycle reactors have been used for determining reaction kinetics, i.e., Berty reactor, Carberry reactor, Robinson-Mahoney reactor, and gradient-less external recycle reactor or jet-loop reactor. Each reactor provides different flow characteristics inside its reactor. All of these are explained in the next section.

2.2.1. Gradient-less internal recycle reactor

Firstly, the gradient-less internal recycle reactors were described. The four common types of gradient-less internal recycle reactors are shown in Figs. 9 and 10 based on the technology of Parker Autoclave Engineers. The Berty stationary basket catalyst testing reactor and the Carberry spinning catalyst basket reactor are designed for gas-solid reaction system. In contrast, Robinson-Mahoney stationary and spinning catalyst basket reactors can be used with gas-liquid-solid (three-phases) reaction systems [49-51]. The Berty reactor is designed with a fixed circular screened catalyst bed and a bottom-mounted vane type blower [52]. The fluid is directed upward along the wall of the vessel in the Berty reactor. After that, it is deflected downward through the fixed catalyst bed [52]. These phenomena generate internal recycling within the Berty reactor [52]. For the Carberry reactor, the characteristic of the catalytic basket is a "cruciform" cross-section. Each arm of cruciform acting as a differential reactor can load the test catalyst and sweep through the fluid of reactants with high speed by rotating shaft [53]. Impellers are installed below and above the cruciform basket in order to direct fluid flow [53]. The basket designs of the Carberry-type reactor are shown in Fig. 11; Flat blade basket (left) and Pitched blade basket (right) [4]. The pitched-type stirrer was claimed that good mixing property was achieved [4, 54]. Remarkably, the disadvantage of the Carberry-type reactor is that the temperature profile of the catalyst bed cannot be measured in this reactor. Thus, highly exo- or endothermic reactions should be avoided for this Carberry reactor because of operating safety.

Subsequently, Robinson-Mahoney stationary catalyst basket reactor, as shown in Fig. 10(a), is a popular reactor design that circulates liquid reactants through a fixed catalyst bed [55]. Impellers (speed up to 1000 rpm) act to draw the fluid into the center of an annular catalyst basket. The prominent points of this reactor are applying with the multiphase reactions (gas-liquid-solid) and permitting to operate in high temperature and pressure conditions. On the other hand, the annular catalyst basket is rotated on a shaft to move the catalyst bed through reactants for the Robinson-Mahoney spinning catalyst basket reactor, as shown in Fig. 10(b) [56]. The baffles inside the annular catalyst basket and the fixed baffles outside this basket control the direction of reactant flow. These high-pressure laboratory apparatuses can be used for catalyst screening, catalyst characterization, and surface chemistry studies in multiphase reactions.
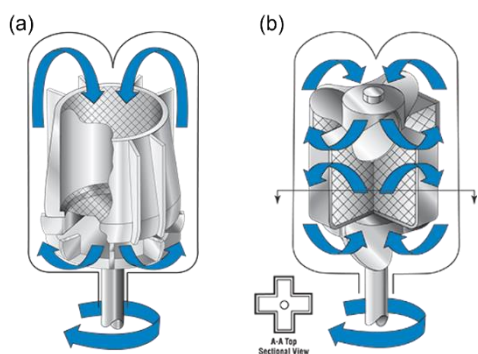
Fig. 9. (a) Berty stationary catalyst basket reactor and (b) Carberry spinning catalyst basket reactor manufactured by Parker Autoclave Engineers [52, 53] (Accessed Aug 14, 2021).
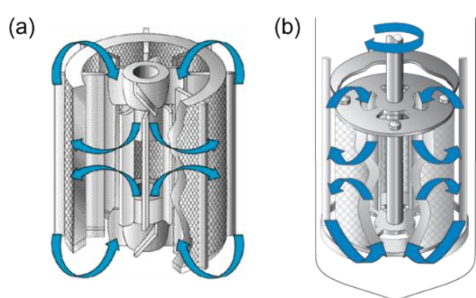

Fig. 10. Robinson-Mahoney (a) stationary and (b) spinning catalyst basket reactors manufactured by Parker Autoclave Engineers [55, 56] (Accessed Aug 14, 2021).
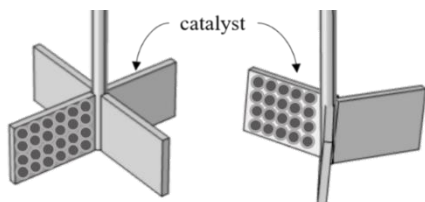

Fig. 11. Basket designs for Carberry-type reactors (Adapted from [4]).

2.2.2. Gradient-less external recycle reactor

Besides the gradient-less internal recycle reactor, the gradient-less external recycle reactors have been investigated for kinetic studies, as shown in Fig. 12 [57-59]. The gradient-less external recycle reactor, as so-called "Jet-loop reactor", is a combination between the differential packed bed reactor and the external recirculation system with the pump. In many cases, the flow meter (such as rotameter) is usually installed at the recycle stream to measure the flow rate. The reactant flow is recirculated through the catalyst bed as same as the phenomena inside the gradient-less internal recycle reactor. Therefore, the flow behavior of the gradient-less external recycle reactor is similar to that of the continuous stirred-tank reactor (CSTR). In addition, this loop reactor can be used to study the details of the elementary reaction sequence for relatively uncomplicated reactions [57]. According to

Ortega et al. (2018), an external recycle reactor was used for the intrinsic kinetic study of methanol to dimethyl ether (DME) conversion over a ZSM-5 catalyst [60]. They found that the true activation energies calculated in their work were close to the values considered by DFT calculations [60].
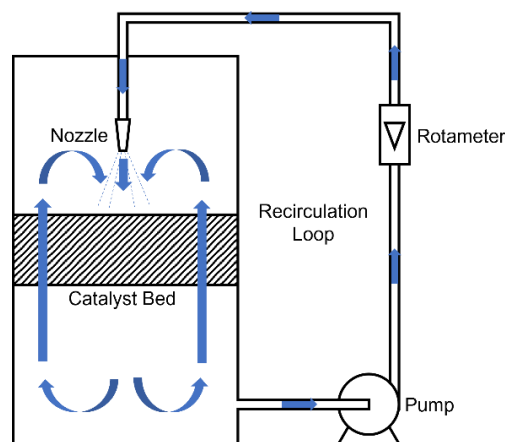

Fig. 12. The schematic diagram of the gradient-less external recycle reactor system.

2.2.3. Development of Gradient-less Recycle Reactor

From the past to present, several research papers indicated that the gradient-less recycle reactors, as mentioned above, have a potential for determining intrinsic kinetics. The applications of gradient-less recycle reactors in previous works with their catalysts were tabulated in Table 1. According to this table, the gradient-less reactor can be applied with various reaction systems such as oxidation, hydrogenation, dehydrogenation, Fischer-Tropsch synthesis, olefins metathesis, etc. Most of them were found that these reaction rates were free from limitations of external- and internal- mass transfer and heat transfer [61-63]. In some cases, they indicated that the activation energy and reaction rate of the gradient-less recycle reactor were higher than these values of other reactors [61, 63]. Moreover, the mixing degree in the gradient-less recycle reactor can be considered as ideal or perfect mixing by testing residence time distribution (RTD) or recycle ratio [61, 64]. However, some researchers have still reported that the non-ideal behavior can be observed in some operating conditions of the gradient-less reactor [65, 66]. Consequently, before measuring intrinsic kinetics, it is crucial to verify the ideality of the reactor with the well-mixed flow and the limitations of all transport processes should be avoided.

Table 1. Applications of the gradient-less reactor, including their used catalysts.

Year	Researcher	Research area	Type	catalysts	Ref.
1975	Choudhary et al.	n-butene isomerization	C	Fluorinated η- Al_2O_3	[67]
1988	Al-Saleh et al.	Ethylene oxidation	B	Ag/α-Al_2O_3	[61]
1992	Hannoun & Regalbuto	Mixing characteristics	B	Ni/Al_2O_3	[9]
1992	Zwahlen & Agnew	Isobutene dehydrogenation	B	$Cr_2O_3/ZrO_2/Al_2O_3$	[68]
1993	Bos et al.	Ethyne/ ethene hydrogenation	B	Pd/Al_2O_3	[62]
1994	Schoenfelder et al.	Methanol to olefins production	B	HZSM-5	[64]
1996	Gomes & Fuller	Propane metathesis	B	Re_2O_7/γ-Al_2O_3 pellets	[69]
2005	Botes	Fischer-Tropsch synthesis	B	HZSM-5	[70]
2015	Azadi et al.	Fischer-Tropsch synthesis	C	Co/γ-Al_2O_3	[71]
2015	Poulopoulos	Ethanol oxidation	C	Pt/Rh, Pd	[72]
2016	Raghuveer et al.	Pyridine hydrogenation (HDN)	B	Sulphided $NiMo/Al_2O_3$	[63]
2017	Fornero et al.	Reverse water gas shift	C	$Ga_2O_3/Cu/ZrO_2$	[73]
2017	Jodlowski et al.	New method for tuning kinetics	B	CoO_x, Pd	[65]
2019	Pretorius et al.	AHF fluorination	C	$Nd_2(CO_3)_3 \cdot H_2O$	[50]
2020	Ountaksinkul et al.	1-butene isomerization	B	MgO	[49]

***B = Berty-type Reactor, and C = Carberry-type Reactor

Al-Saleh et al. (1988) studied the intrinsic kinetics of ethylene oxidation reaction over a commercial Ag/α-Al_2O_3 catalyst under industrial conditions in an original Berty-type reactor established by J.M. Berty of Union Carbide and manufactured by Autoclave Engineers, Inc (as shown in Fig. 9(a)) [61]. The effect of impeller speed on the reaction rate at different temperatures was studied to identify the limitation of external mass diffusion [61]. They found that increasing the number of revolutions per minute (impeller speed) slightly affected reaction rates under all temperatures. Therefore, they could indicate that the external mass transfer resistance was insignificant. For internal mass diffusion, a common method to study pore diffusion is to reduce the particle size of the catalyst [74]. Unfortunately, if the particle size of the catalyst is too small, it cannot be packed in the gradient-less internal recycle reactors (such as the Berty-type and Carberry-type reactors). The catalyst loss can occur in these reactors. Therefore, the theoretical criterion was used to investigate the pore diffusion instead of the method above. The criterion of Weisz and Hicks could be used as shown in Eq. (1).

$$\phi = \frac{r_{obs}\rho_c R^2}{C_b D_e}\left[exp\left(\frac{\gamma\beta_T}{1+\beta_T}\right)\right] \qquad (1)$$

If $\phi < 1$, the internal mass transfer can be neglected. Under the maximum temperature of the predetermined range (553 K) in the research of Al-Saleh, ϕ was equal to 0.19; therefore, they summarized that there was no internal mass transfer in their Berty reactor [61]. Besides, the theoretical criteria are usually used to investigate the limitations of external- and internal- mass transfers as well as limitation of heat transfer, as more described in the section 4.

For the heat transfer, the advantage of the Berty-type reactor over the Carberry reactor is that the temperature profile throughout the catalyst bed can be measured. Thus, the heat transfer limitation can be observed in the Berty reactor by measuring the temperatures at the top and bottom of the catalyst bed. The measured temperature difference across the catalyst bed was in a range of 0.5 to 2 °C in the research of Al-Saleh, therefore the heat transfer resistance in their Berty reactor can be neglected [61]. According to Ountaksinkul et al. (2020), the temperature profile along the catalyst bed was also measured in the Berty reactor at a set point temperature of 400 °C [49]. The observed temperature difference between the top and bottom bed was also within 2 °C.
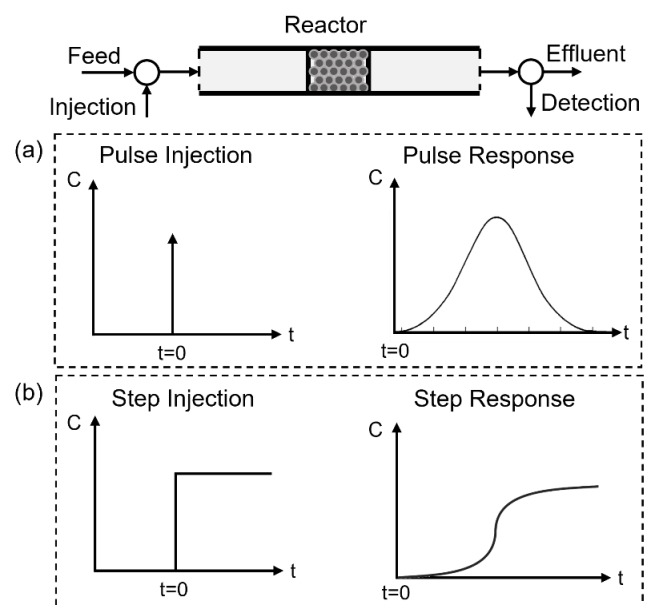
Fig. 13. The initial RTD curve and response of (a) pulse input and (b) step input from the tracer experiment.

To verify the ideality of the Berty reactor, the recycle ratio inside this reactor was investigated. Al-Saleh et al. found that the recycle ratio at an impeller speed of 950 rpm used in their research was equal to 53 [61]. The minimum recycles ratio estimated by the research of Berty, which provides ideal mixing characteristics, was equal to

20 [75]. Therefore, it was summarized that their operating conditions in the Berty reactor performed excellent mixing characteristics. Moreover, their results showed that their activation energies for the partial and complete oxidation reactions of ethylene over silver catalysts were higher than the previous studies. The activation energies for the reaction rate of ethylene oxidation in their work was 95 kJ mol^{-1}, whereas the activation energies in previous works ranged from 35.4 to 90 kJ mol^{-1}. It was due to the absence of all transport limitations and the perfect mixing. Consequently, the calculated reaction rates of Al-Saleh et al. corresponded to their experimental reaction rates.

Then, Hannoun and Regalbuto (1992) studied the mixing characteristics in a micro-Berty catalytic reactor, as shown in Fig. 14 [9]. All components of this micro-Berty reactor were tabulated in Table 2. It was identical to the original Berty reactor mentioned above but smaller. The reactor was made of 316 stainless steel and Hastelloy C and the catalyst basket has a volume of 3.6 cm^3. The maximum pressure, temperature, and impeller speed limits are 34 atm, 450 °C, and 5000 rpm, respectively. The bulk and internal gas-phase mixing characteristics of the micro-Berty catalytic reactor had been evaluated by the stimulus-response technique to determine the residence time distribution (RTD) [9]. Figure 13 shows the initial and response RTD curves for the two cases of pulse input (Fig. 13(a)) and step input (Fig. 13(b)). Both injections are the most common methods for the tracer experiment and easier to interpret data. For pulse injection, a tracer is instantaneously introduced into the fluid entering the vessel, whereas the ordinary fluid is switched to the fluid with a steady tracer flow for a step input.

According to Hannoun and Regalbuto (1992), the stepwise change of 3% H_2/N_2 concentration of tracer was applied with the constant volumetric flow rate (Q) at 12.8 cm^3 min^{-1} [9]. The measurement was taken for 8 minutes and sampled every 1 minute. The effects of impeller speed, temperature, pressure, flow rate, and catalyst particle size of the micro-Berty reactor on the mixing characteristics were investigated [9]. It was found that both flow rate and pressure significantly influenced the tracer concentration responses. Low gas density led to poor internal recycling inside the reactor and well-mixed flow could be observed at the pressure above 6.80 atm and impeller speed of 1000 rpm. Furthermore, all particle shapes slightly affected concentration-response or mixing characteristics. The effective volume was estimated to be 3.4 cm^3, which had an excellent agreement with the real volume of the catalyst basket (3.6 cm^3) and did not have a dead volume at pressures above 6.8 atm. Whereas, the effect of impeller speed was found that the external mass transfer limitation existed at 1/T below 0.002 (1/K) and the perfect mixing was achieved above 1000 rpm in their research. Although many researchers confirmed that the absence of mass- and heat- transfer limitations and well-mixed flow were provided inside the gradient-less recycle reactor, these resistances can probably appear in some operating conditions. Remarkably, the poor mixing characteristics can occur at atmospheric pressure for the Berty reactor.
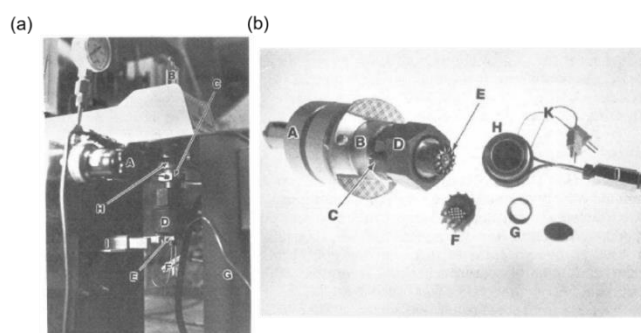

Fig. 14. (a) The micro-Berty catalytic reactor and (b) components of reactor assembly of Hannoun and Regalbuto. (Reprinted (adapted) with permission from [9]. Copyright (1992) American Chemical Society.)

Table 2. List of components in the micro-Berty catalytic reactor [9].

Reactor and stand (a)		Components of reactor assembly (b)	
A	back-pressure regulator	**A**	magnetic drive
B	magnetic drive	**B**	magnetic-drive cooling jacket
C	outlet and inlet	**C**	outlet and inlet
D	heater and internal cooling coil	**D**	flange nut
E	bottom of the reactor vessel	**E**	impeller
F	thermocouples	**F**	vaned catalyst basket
G	reactor stand	**G**	diffuser ring
H	magnetic-drive cooling jacket	**H**	reactor vessel
I	hold-back wrench	**I**	reactor cooling coil
-	-	**K**	Thermocouples

Besides the residence time distribution (RTD) study, the determination of the recycle ratio, as mentioned in Al-Saleh et al. [61], can also be used to investigate the flow characteristics inside the gradient-less recycle reactors. According to Warnecke et al. (2020), kinetic investigations of olefins interconversion reactions with a commercial H-ZSM-5 catalyst were also performed using a gradient-less and isothermal Berty-type reactor integrated with a high-performance online gas chromatography [76]. A flow probe with a diameter of 3 mm was installed inside the catalyst basket to consider whether their Berty reactor was working properly. The gas fluid in the catalyst basket was slightly disturbed by this probe due to the high diameter of the basket to probe ratio. A thermal principle was used to measure gas velocities, as called "heat ball". The measured velocity corresponded to the volumetric flow of the recycle stream. For their experiments, the recycle to feed volumetric flow ratio should be greater than 50 to

achieve perfect mixing. According to Brosius and Fletcher (2010), the direct measurement of recycle ratio in internal recycle laboratory reactor was described intensely [77]. Remarkably, this method with the flow probe is quite complicated and may disturb the fluid flow inside the catalyst bed in the gradient-less recycle reactor. Before performing this method, it is important to ensure that the system is not affected by the flow probe.

On the other hand, according to Ountaksinkul et al. (2021), the flow characteristics of the Berty reactor can be investigated by computational fluid dynamics (CFD) simulation [78]. The CFD simulation could clearly observe the transport phenomena and the location of the dead zone inside the Berty reactor. Moreover, percentages of bypassing and dead zone inside the Berty reactor can be estimated by these CFD results with parameter estimation. This leads to the suitable determination of the perfect mixing region without the disturbance of the flow probe. The perfect mixing region with the dead zone and bypassing below 1% inside the original Berty reactor could be found at pressures above 6 atm, impeller speeds above 1896 rpm, and mass flow rates above 1.48×10^{-6} kg s^{-1} [78]. This operating window corresponded to the well-mixed region from Hannoun and Regalbuto (1992) [9].

Owing to the limitation of using gradient-less recycle reactor at atmospheric pressure or relatively low pressure with poor mixing characteristics, several researchers have attempted to develop a new design of the Berty reactor to expand the operating window with the perfect mixing. Figure 15(a) shows the layout of the RotoBerty reactor, in which catalyst was packed in the inner tube to avoid local maldistribution and catalyst by-passing [1]. Several designs of stirrer provide well-mixed flow, although two-stage turbines are adopted. These designs can expand the maximum impeller speed up to 10,000 rpm. The stirrer is often driven by feedthrough of the stirrer axis or by magnetic coupling; however, the leakages and the existence of dead-zone area should be concerned in these designs [1].
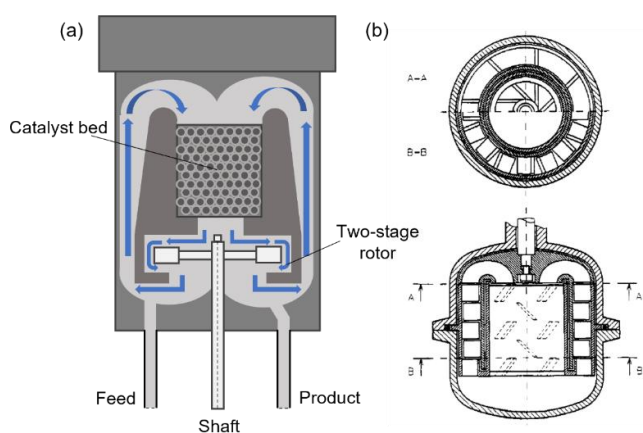

Fig. 15. (a) RotoBerty reactor and (b) modified Berty reactor with the three-stage turbine. (Reprinted (adapted) with permission from [68]. Copyright (1992) American Chemical Society.)

Zwahlen and Agnew (1992) found that the standard Berty gradient-less reactor could be successfully modified for operating up to 600 °C and at atmospheric pressure without all transport resistances [68]. To improve the gas mixing, the characteristics of the modified Berty reactor were shown in Fig. 15(b) and the two main modifications were applied as below [68]:

1. A maximum shaft speed of the air motor was improved by a direct-flanged three-phase motor (0.55 kW) to enhance the maximum shaft speed from 2500 rpm to 4500 rpm.

2. The original 8-blade single-stage turbine of the standard Berty reactor was replaced by a specially designed three-stage turbine. The flow guiding channel was designed with enlarged vanes positioned at an angle of 45° to reduce internal drag force. The two axial stages with 8 vanes at 45° were incorporated. The static vanes were set at the outlet of each stage. In addition, a complex labyrinth was used in the system to reduce the internal backflow.

These modifications mentioned above can improve the generated pressure head from the original design. The 3-Stage turbine provides a higher generated pressure head than other stirrer designs. Their results from the tracer experiment indicated that the perfect mixing could be assumed at impeller speeds of 2000 and 3000 rpm near atmospheric pressure. They recommended that their modified Berty reactor can handle the maximum temperature up to 600 °C and the pressure close to 1 atm with well-mixed behavior.

Recently, a new design of the Berty reactor, as shown in Fig. 16, was developed in 2014 and it is known as the "ILS-Berty internal recycle reactor". The patent of this reactor is the exclusive licensing agreement between Integrated Lab Solutions (ILS) and Friedrich-Alexander University, Erlangen, Germany [79]. The current assignee claimed that this invention could provide a next-generation Berty reactor for the kinetic studies of heterogeneous catalytic reactions (gas-solid reactions) at low-to-medium pressures. The reactor was modified to be more compact and completely eliminated the need for an external motor with rotating parts [79, 80]. The use of a novel electromagnet can allow the stirring rate to 10,000 rpm [80]. Due to the high speeds and abandonment of moving parts, it offers a broader pressure operating window. Furthermore, the drive motor was installed at the top of this Berty reactor in contrast to the original Berty reactor, in which the motor and the impeller are usually placed at the bottom of the catalyst bed. The cooling system was also used to remove generated heat from the motor. In summary, the state-of-the-art ILS Berty reactor can be used to investigate intrinsic catalyst properties suitably without all transport limitations and provide the perfect mixing region under testing conditions at high temperatures up to 600 °C and atmospheric pressure or nearby.
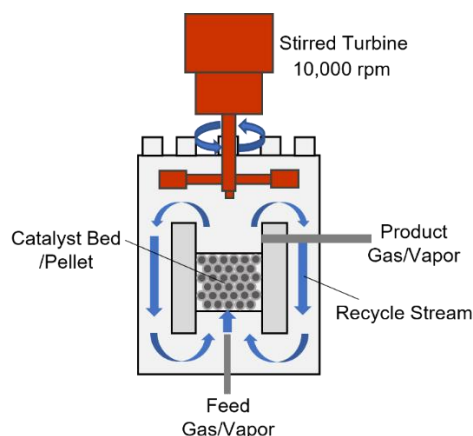
Fig. 16. ILS Berty internal recycle reactor.

According to Ountaksinkul et al. (2020), the schematic diagram of the experimental apparatus for 1-butene isomerization in a gradient-less recycle reactor (Berty-type reactor) was described, as shown in Fig. 17 [49]. Before the beginning, the leakage should be checked to avoid toxic emissions during the reaction and reduce the experimental error. Then, the reactant flow rate should be ensured that it was fed at a steady flow rate by analyzing the feed components at the bypass stream. In many cases, the reactant flow was preheated to ensure that the reactant was fed under desired operating conditions with a single-phase and isothermal condition [81]. Whereas, for product

stream, the liquid product should be separated in some cases before being analyzed by detector units such as gas chromatography. During the experiment, the cooling system should be provided to remove generated heat from the rotation of the motor. After catalyst testing at the different conditions, these experimental kinetic data were regressed with the mathematical models to determine the kinetic parameters involving activation energies, pre-exponential coefficients, adsorption, and desorption coefficients. As mentioned above, if the perfect mixing and the absence of all transport limitations were provided, these kinetic parameters could represent the intrinsic kinetics in the gradient-less recycle reactor suitably. In addition, the errors of equipment should also be calculated in the parameter regression to provide reliable kinetic information [81].

In addition, according to Jodłowski et al. (2017), a new numerical method for separating the intrinsic kinetics from the mass diffusion effect in the gradient-less recycle reactor was proposed [65]. They found that the observed reaction rate in the gradient-less recycle reactor can probably be limited by the diffusion effect at low temperature even under high mixing conditions owing to catalyst activity and the structured geometry of the catalyst carrier. Their equations for determining intrinsic kinetics were shown in the following section of intrinsic kinetic modeling.
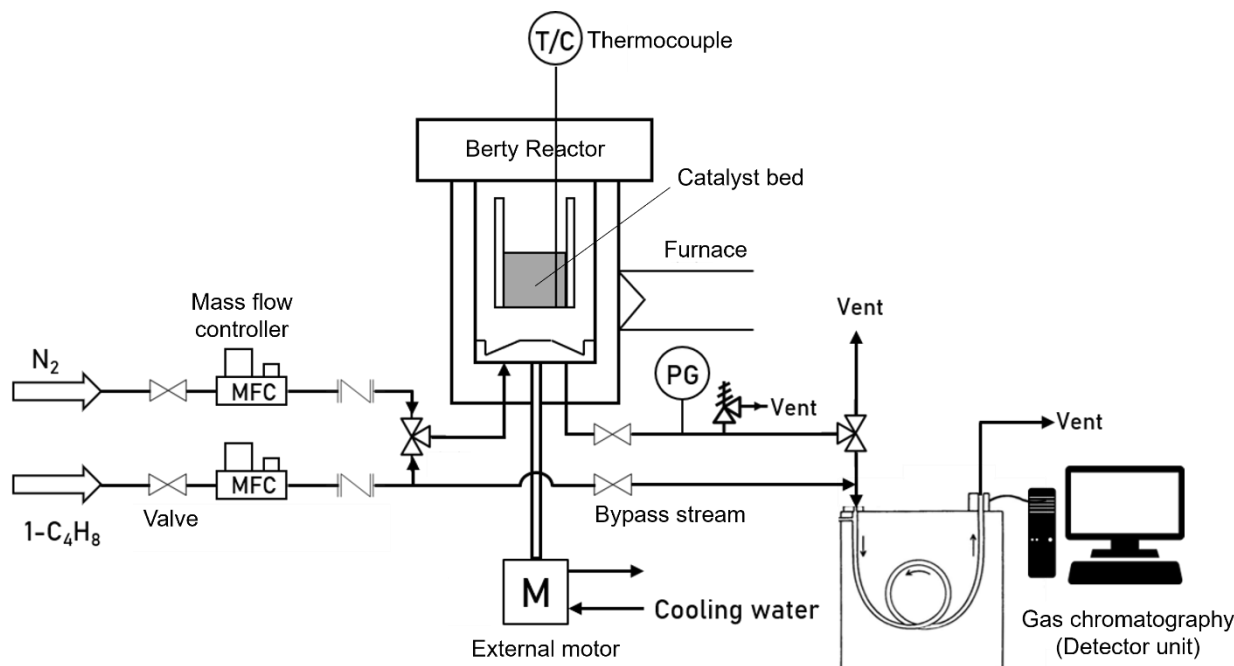
Fig. 17. Typical Berty reactor system used to determine reaction kinetic parameters.

3. Intrinsic Kinetic Modeling

Based on the knowledge of catalytic reaction engineering, intrinsic kinetic modeling is inseparably related to transport phenomena, reaction mechanisms, and reactor engineering [1]. The mass, heat, and momentum balance equations, rate expressions of

chemical reactions (Power law, or LHHW), and parameter estimation are performed to achieve the kinetic parameters. Generally, operating variables of the reactor (flow rate, catalyst amount, temperature, etc.) were studied together with a consideration of conversion or reaction rate. Due to the different types of reactors as mentioned in section 2, intrinsic kinetic modeling for each reactor is

different depending on the reactor studied. In this section, various models for determining intrinsic kinetics of the two common-used reactors, i.e., gradient-less recycle reactor and plug flow reactor, were more described.

3.1. Kinetic Modeling for Gradient-less Recycle Reactor

3.1.1. Ideal CSTR Model

As the flow characteristics inside the gradient-less recycle reactor and continuous stirred-tank reactor (CSTR) are identical, various CSTR models can represent the gradient-less recycle reactor as well. Firstly, the general mole balances for a component i, as shown in Eqs. (2) and (3), are applied for the catalyst bed with assuming isothermal conditions and neglecting the pressure drop across the bed. Under steady-state operation, the accumulation term can be neglected.

$$in - out + generation - consumption$$
$$= accumulation \qquad (2)$$
$$F_{i0} - F_i + \int_V r_i dV = \frac{dN_i}{dt} \qquad (3)$$

For the gradient-less recycle reactor and CSTR, the perfect mixing inside these reactors is assumed for ideal cases; therefore, the volume (V) can be considered as a constant. The general mole balance for a component i above can be rewritten to the simple algebraic equation below.

$$F_{i0} - F_i = -r_i' W \qquad (4)$$

where F_{i0} and F_i are the mole flow rate (mol s⁻¹) of species i at inlet and outlet of the reactor, whereas r_i and r_i' are reaction rate per volume (mol m⁻³ s⁻¹) and weight of catalyst (mol g-cat⁻¹ s⁻¹). V and W are the volume of the reactor (m³) and weight of catalyst (g), respectively. This model can be used to estimate intrinsic kinetics in the case, in which the limitations of mass- and heat- transfers were eliminated entirely and the perfect mixing was verified.

For the rate of reaction term (r_i), the rate expression can be provided by various model types. According to Bos et al. (1997), the kinetic models can be briefly classified into five types; 1. Simple first order or Power-law, 2. Langmuir Hinshelwood Hougen Watson (LHHW), 3. N-lumped models (for complex systems), 4. Detailed mechanistic model, and 5. Ab initio, molecular dynamics [82]. Nevertheless, Power-law and Langmuir Hinshelwood Hougen Watson (LHHW) are the most common models for kinetic modeling due to the easiness of integration into the reactor model. For the simplest method, the Power-law model can be written in Eqs. (5) and (6) for the irreversible and reversible gas-phase reactions ($A + B \rightarrow C$), respectively.

$$r_{i,irrev} = k p_A^m p_B^n \qquad (5)$$

and

$$r_{i,rev} = k_f p_A p_B - k_b p_C \qquad (6)$$

where p_i is the pressure of each species. k_f and k_b are the kinetic constants for forward and reverse reaction rates, respectively. An Arrhenius-type expression is the most common form for k, as shown in Eq. (7).

$$k = A_0 exp(-E_a/R_G T) \qquad (7)$$
$$K_{eq} = \frac{k_f}{k_b} \qquad (8)$$

where E_a is activation energy (kJ mol⁻¹), A_0 is the pre-exponential factor, R_G is a gas constant (8.314, J mol⁻¹ K⁻¹), and T is a temperature. k_f and k_b relate to equilibrium constant (K_{eq}) as shown in Eq. (8).

For Langmuir Hinshelwood Hougen Watson (LHHW), it is one of the most popular and simple methods to approach reaction kinetics. This model combines the physical and chemical processes occurring at the catalyst surface (including adsorption and desorption processes) into the mathematical rate expression, as shown in Eq. (9). The accuracy of rate expression for LHHW relates to selecting the appropriate rate-determining step. The rate-determining step can be ad-, desorption of the components, or the surface reaction. Moreover, the rate-determining step affects the estimation of kinetic parameters and parameter fitting. Therefore, the choice of the rate-determining step is very essential. The studies about reaction mechanisms and associated areas can support the researchers in considering the proper rate-determining step.

$$rate \quad \alpha \quad \frac{(kinetic\ factor)(driving\ force)}{(adsorption\ term)^n} \qquad (9)$$

3.1.2. Non-ideal CSTR Model

Frequently, a recycle ratio is recommended that it should be greater than 20 for ideal-mixing of the gradient-less recycle reactor but this criterion is not suitable for all cases [61]. The recycle ratio is not a fixed value but depends on conversion level and others as described in the literature [83]. According to Warnecke et al. (2020), they investigated the recycling in their Berty-type reactor with a flow probe and the two balancing concepts assuming the Berty reactor with ideal CSTR or PFR with recycle stream [76]. Their new concept of flow characterization and simulation revealed that the recycle to feed volumetric flow ratio should be greater than 50 for their Berty-type reactor. If the recycle ratio of gradient-less recycle reactor is improperly defined, the non-ideal flows such as dead-zone or channelling can be occurred in the gradient-less recycle reactor. Therefore, the non-ideal CSTR model including parameters of the dead-zone and bypassing is possible to be another method for the determination of intrinsic kinetics.
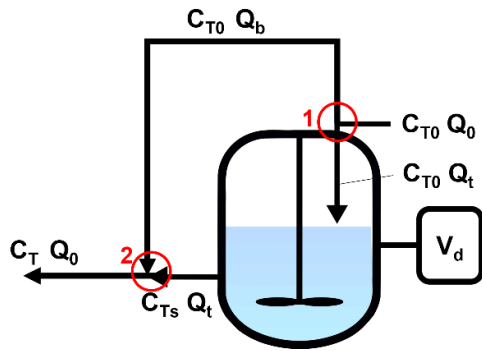
Fig. 18. Non-ideal CSTR model with dead-zone and channeling (Adapted from [84]).

According to Conesa (2020), the flow diagram of this system is shown in Fig. 18 [84]. The non-ideal CSTR model was created with the combination of non-stationary and stationary volumes and channeling flow. When considering the mixing point of bypassing and effluent streams (at point 2), the mole balance around this point can be defined as Eqs. (10) and (11).

$$C_{T0}Q_b + C_{Ts}Q_t = C_T(Q_b + Q_t) \qquad (10)$$

$$C_T = \frac{C_{T0}Q_b + C_{Ts}Q_t}{Q_0} \qquad (11)$$

If we define:

$$\alpha = \frac{V_t}{V}, \qquad \beta = \frac{Q_b}{Q_0}, \text{ and } \tau = \frac{V}{Q_0} \qquad (12)$$

where Alpha (α) is a fraction of non-stationary regime to total volume, whereas Beta (β) is a fraction of short-circuiting or bypassing to total volumetric flow rate. The exit concentration (C_T) can be rewritten as Eq. (13).

$$C_T = \beta C_{T0} + (1 - \beta)C_{Ts} \qquad (13)$$

When a 1st order reaction is assumed, a mole balance on the non-stationary volume (V_t) of the reactor can be given by Eqs. (14) and (15):

$$C_{T0}Q_t - C_{Ts}Q_t - kC_{Ts}V_t = 0 \qquad (14)$$

$$C_{Ts} = \frac{C_{T0}(1 - \beta)Q_0}{(1 - \beta)Q_0 + \alpha Vk} \qquad (15)$$

When substituting Eq. (15) into Eq. (13), the effluent concentration can be given, as shown in Eq. (16).

$$\frac{C_T}{C_{T0}} = \beta + \frac{(1 - \beta)^2}{(1 - \beta) + \alpha\tau k} \qquad (16)$$

Therefore, if the initial concentration (C_{T0}), the exit concentration (C_T), and the parameters for determining dead-zone (α) and channeling (β) can be defined; Equation (16) can be used as a mathematical model to determine intrinsic kinetic parameters. These parameters

for determining dead-zone (α) and channeling (β) can be obtained from the tracer experiment. For example, according to Jafari and Mohammad-Zadeh (2005), a gas-induced contactor was modeled by the non-ideal CSTR model mentioned above with the residence time distribution (RTD) experiments [85]. Their analysis showed that both dead-zone and channeling in their system could be quantitatively investigated. A dead zone of 16.7% can be observed at a low liquid flow rate, while bypassing at a high flow rate was 10 %. The quantities of dead-zone and channeling from these tracer experiments are applicable to Eq. (16).

In addition, this non-ideal CSTR model with dead-zone and bypassing can be adopted with the mole balance of the tracer experiment. The exit-age distribution (E-curve, or RTD-curve) can be defined as shown in Eq. (17).

$$E(t) = \frac{(1 - \beta)^2}{\alpha\bar{t}} \cdot exp\left[-\frac{1 - \beta}{\alpha}\left(\frac{t}{\bar{t}}\right)\right] \qquad (17)$$

3.1.3. CSTR Model with Mass Diffusion

In some cases, the mass diffusion can also significantly affect intrinsic kinetic modeling for gradient-less recycle reactors. Although the gradient-less recycle reactor is operated under high mixing conditions, the reaction rate can be limited by the effect of mass diffusion at low temperature due to structured catalyst carrier geometry [65]. To extract intrinsic kinetics from the effect of mass diffusion, Jodlowski et al. (2017) proposed a new method to determine intrinsic kinetics and mass diffusion parameters in a gradient-less recycle reactor [65].

The balance of mass transfer of reactant A to catalyst surface and 1st order reaction at catalyst surface was shown as below:

$$k_c(C_A - C_{As}) = k_r C_{As} \qquad (18)$$

where k_c is mass transfer coefficient (m s-1), k_r is intrinsic kinetic constant (mol s-1), C_A and C_{As} are the concentration of A in the bulk gas phase and at catalyst surface (mol m-3), respectively. The concentration at catalyst surface (C_{As}) can be rewritten in the equation below:

$$C_{As} = \frac{k_c}{k_c + k_r}C_A \qquad (19)$$

Combining Eqs. (18) and (19) gives:

$$-r_A = k_{app}C_A = k_r C_{As} = \frac{k_r k_c}{k_r + k_c}C_A = \frac{1}{\frac{1}{k_c} + \frac{1}{k_r}}C_A \quad (20)$$

The equation above shows that the measured kinetic constant can be governed by mass transfer resistances ($1/k_c$) and the reactive resistances ($1/k_r$). Therefore, the overall rate of reaction can be considered for two cases. First, the mass transfer limitation can be neglected, and the intrinsic kinetics is a rate-determining step, as shown in Eq.

(21). Second, Eq. (22) shows that the observed reaction rate is limited by mass transfer, whereas the intrinsic kinetics is dominated.

$$k_c \gg k_r : -r_A = k_r C_A \qquad (21)$$
$$k_r \gg k_c : -r_A = k_c C_A \qquad (22)$$

To estimate the intrinsic kinetic constant (k_r) from the experimental data, Eq. (20) was rearranged into Eq. (23), and the apparent kinetic constant (k_{app}) can be provided by the set of experimental results.

$$k_r = \frac{k_{app} k_c}{k_c - k_{app}} \qquad (23)$$

To describe the mass transfer coefficient (k_c), the general equation for mass transfer in various packings was proposed by Hobler (1962) as below [86]:

$$Sh = 0.11 \, Re^{0.8} \, Sc^{1/3} \qquad (24)$$

However, the correlation for mass transfer coefficient depends on fluid phase, packing type, flow regime, etc. [87-89]. Equation (24) can be rewritten into Eqs. (25) and (26). The mass transfer coefficient was expressed as below [65]:

$$\left(\frac{k_c d}{D_A}\right) = 0.11 \left(\frac{wd\rho}{\mu}\right)^{0.8} \left(\frac{\mu}{\rho D_A}\right)^{1/3} \qquad (25)$$

$$k_c = 0.11 w^{0.8} d^{-0.2} \left(\frac{\rho}{\mu}\right)^{0.47} D_A^{2/3} \qquad (26)$$

For D_A, ρ, and μ, these parameters are a function of the reaction temperature (T) and can be calculated by using Gilliland, Sutherland, and Clapeyron equations, respectively [65, 86]. Therefore, the formula of mass transfer coefficient as a function of temperature (T) can be given by:

$$k_c = 0.11 w^{0.8} d^{-0.2} D_{A0}^{2/3} \left(\frac{\rho_0}{\mu_0}\right)^{0.47}$$
$$T_0^{0.175} \left[\left(T^{-2.5} \frac{T + 114}{T_0 + 114}\right)^{0.47} T \right] \qquad (27)$$
$$= B \left[\left(T^{-2.5} \frac{T + 114}{T_0 + 114}\right)^{0.47} T \right]$$

In summary, the observed reaction rate may be influenced by the external mass transfer in a gradient-less recycle reactor. If the effect of mass diffusion is significant, the intrinsic kinetics cannot be observed. After the apparent kinetic constants (k_{app}) were obtained from the kinetic experiments, Eq. (23) can be used to determine the intrinsic kinetic constant (k_r) with Eq. (27) to calculate mass transfer coefficient (k_c). Moreover, the two constraints in Eqs. (21) and (22) can define the rate-determining step between mass diffusion and chemical kinetic controls. From their results, the Arrhenius plots of

$\ln(k_r)$ and $1/T$ performed an excellent linear relationship between both parameters.

3.2. Kinetic Modeling for Packed Bed Reactor

According to the general mole balance, as shown in Eq. (2), it can be rewritten for ideal plug flow reactor under steady-state condition for species A as shown in Eq. (28)

$$\frac{dF_A}{dW} = r_A' \qquad (28)$$

where F_A is the flow rate of component A (mol s⁻¹) and r_A' is the reaction rate (mol g-cat⁻¹ s⁻¹). Normally, the fluid flow through the packed bed reactor affects pressure drop inside the tube. To operate in isobaric condition, the particle diameter (d_p) should be carefully considered. If the particle size is too small, pressure drop can be significant for the packed bed reactor. Consequently, the addition equation (such as the Ergun equation [90]) should be coupled in the reactor model as the equation below.

$$\frac{\Delta P}{L} = \frac{150\mu(1 - \varepsilon_b)^2 u_0}{\varepsilon_b^3 d_p^2} + \frac{1.75(1 - \varepsilon_b)\rho u_0^2}{\varepsilon_b^3 d_p} \qquad (29)$$

where ΔP is the pressure-drop (atm), L is the bed length (m), μ is the fluid viscosity (Pa s), ε_b is the void fraction of the bed, u_0 is the superficial fluid velocity (m s⁻¹), d_p is the particle diameter (m), and ρ is the fluid density (kg m⁻³).

Besides the ideal plug flow model, some research papers show that the axial dispersion model, as shown in Eq. (30), was used for kinetic modeling [91, 92]. When the reactor diameter to catalyst particle diameter ratio (D/d_p) is lower than 10, the axial dispersion is dominant [13]. In addition, when the catalyst bed length to particle diameter ratio (L/d_p) is less than 50, the axial change of reactant partial pressure can be found as well.

According to Kangas et al. (2008), the axial dispersion reactor (ADR) model coupled with the Ergun equation was used to determine the kinetic parameters of skeletal 1-butene isomerization over H-TON and H-FER catalysts [91]. This ADR model provides a simple description for a non-ideal flow behavior deviating from ideal plug-flow and complete back-mixing in the packed bed reactor. From their results, the skeletal isomerization of n-butene can be accurately described by this developed kinetic and reactor model.

$$\frac{\partial C_i}{\partial t} - \frac{\rho_c}{\varepsilon}(1 - \varepsilon_b)C_t r_i = D_{ax}\frac{\partial^2 C_i}{\partial z^2} - \frac{u_s}{\varepsilon}\frac{\partial C_i}{\partial z} \qquad (30)$$
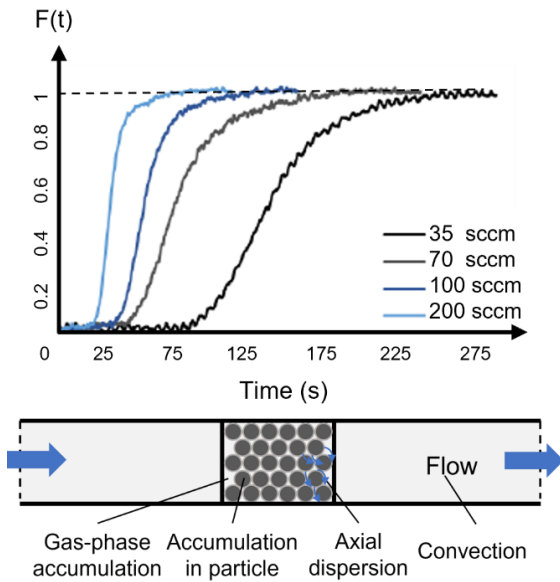
Fig. 19. Experimental RTD curves at different flow rate (Bed void= 0.45, Temperature 298 K) in packed bed reactor [111].

In addition, in our research, the residence time distribution (RTD) experiments were carried out using the stepwise change of helium (He) tracer in the packed bed reactor, as shown in Fig. 19. It was clearly found that the RTD curves at the different feed flow rates deviated from the ideal plug-flow behavior in the fixed bed reactor, especially at a relatively low flow rate. Therefore, a set of continuity equations with axial dispersion term (D_{ax}) is a better choice to extract intrinsic kinetic data from experimental results in the fixed bed reactor for this case, which cannot avoid these dispersions. Under transient operation, the axial dispersion model was performed in the partial differential equation (PDE), as shown in Eq. (30), including four main terms: gas-phase accumulation term, reaction rate term, axial dispersion term, and convection term, respectively. The overall rate of reaction (r_i) can be calculated from the rate of reaction steps considered in the reaction mechanism as shown in Eq. (31).

$$r_i = \sum_p v_{i,p} r_{i,p} \qquad (31)$$

where $v_{i,p}$ is a stoichiometric number of the component i in reaction step p and $r_{i,p}$ is the reaction rate of the elementary step p. For boundary conditions of the axial dispersion model, it is usually assumed to be closed vessel behavior. Thus, initial condition, inlet, and outlet conditions can be given by:

$$t = 0, z \geq 0 \quad C_i = 0 \qquad (32)$$

$$z = 0, t > 0 \quad D_{ax}\frac{\partial C_{i(z=0)}}{\partial z} = -u_s\left(C_{i,0} - C_{i(z=0)}\right)(33)$$

$$z = L, t > 0 \quad \frac{\partial C_{i(z=L)}}{\partial z} = 0 \qquad (34)$$

For axial dispersion coefficient (D_{ax}), it can be generally calculated by the dimensionless term of Péclet

number (Pe). According to Fogler (1999), the definition of Pe is the ratio of the contributions to mass transport by convection to those by diffusion, as shown in Eq. (35) [93].

$$Pe = \frac{Rate\ of\ transport\ by\ convection}{Rate\ of\ transport\ by\ diffusion\ or\ dispersion}$$
$$= \frac{uL}{D_{ax}} \qquad (35)$$

Table 3. Correlations for determining axial dispersion coefficient in fixed bed [94].

Literature	Correlations	Ref.
Hiby et al. (1962)	$1/Pe_p = \dfrac{0.65}{1 + 7\sqrt{\varepsilon_b/(Re\,S\,c)}} + \dfrac{0.67\varepsilon_b}{Re\,S\,c}$	[94, 95]
Chung & Wen (1968)	$\varepsilon_b Pe_p = 0.2 + 0.011 Re^{0.48}$	[94, 96]
De Ligny (1970)	$1/Pe_p = \dfrac{0.7D_m}{2R_p v} + \dfrac{1}{0.4 + 1.76D_m/(R_p v)}$	[94, 97]
Han et al. (1985)	$Pe = 4.36\left(\dfrac{Re\,S\,c}{1-\varepsilon_b}\right)^{-0.262}$	[94, 98]
Athalye et al. (1992)	$Pe_p = \left(\dfrac{1-\varepsilon_b}{Re\,S\,c}\right)^{1/6}$	[94, 99]
Rastegar & Gu (2017)	$1/Pe_p = \dfrac{0.7D_m}{2R_p v} + \dfrac{\varepsilon_b}{0.18 + 0.008Re^{0.59}}$	[94]

Normally, the reciprocal of Pe (D_{ax}/uL) is also used to explain the axial dispersion, as the so-called "Vessel dispersion number". The Péclet number (Pe) is a function of the Reynolds number (Re) and Schmidt number (Sc). Therefore, several researchers have attempted to develop the Péclet number correlations with Re and Sc numbers to estimate axial dispersion coefficient (D_{ax}), as shown in Table 3.

According to Rastegar and Gu (2017), the Péclet number correlation for fixed-bed columns packed with particles was improved [94]. In previous works, some cases did not include the molecular diffusion term and the bed void fraction term. On the other hand, the Péclet number correlation of Rastegar and Gu (2017), based on additional experimental data in the literature, considered both molecular diffusion and bed void fraction; therefore, their correlation is more effective and comprehensive than the others [94].

Recently, according to Sripinun et al. (2021), a one-dimensional axial dispersion model, as shown in Eq. (30), was applied with the mass transfer from the fluid bulk phase to the catalyst pellet under steady-state conditions; therefore, this equation was rewritten into Eq. (36) [100].

$$0 = D_{ax}\varepsilon_b \frac{\partial^2 C_i}{\partial z^2} - u_s \frac{\partial C_i}{\partial z} - (1-\varepsilon_b)\,S_i \quad (36)$$

$$S_i = a_c k_{c,i} \left(C_{p,i} \big|_r - C_i \right) \qquad (37)$$

where a_c is area per volume ratio of catalyst particle (m^{-1}), $k_{c,i}$ is external mass transfer coefficient (m s^{-1}), and $C_{p,i}$ is the concentration of species i at catalyst pellet (mol m^{-3}). For the pellet model, the internal mass transfer in pore structure is often explained by effective pore diffusion and tortuosity models [101]. For this case, the convective term in the mass balance equation can be assumed to be insignificant, accounting for Fickian diffusion and reaction terms. Consequently, the general reaction-diffusion equation of a single catalyst spherical particle is formulated as:

$$0 = D_{e,i} \left(\frac{\partial^2 C_{p,i}}{\partial r^2} + \frac{2 \partial C_{p,i}}{r \partial r} \right) + \rho_c r_i \qquad (38)$$

These equations can be used to describe the packed bed reactor with both axial dispersion and mass diffusion simultaneously. Besides intrinsic kinetic modeling, it can be used to represent the reactor model, including both internal and external mass diffusion.

4. Methods for Determining Mass- and Heat-Transfers

For determining intrinsic kinetics, the limitations of mass- and heat- transfers must be excluded to reveal only chemical reactions on the catalyst surface. However, during the catalytic process, heat consumption or generation due to endothermic/exothermic reactions and external and internal mass diffusions. Consequently, the observed reaction rate from the experiments can be dominated by these limitations. The various experimental methods and criteria for determining mass- and heat-transfers in the kinetic experiment were described in this section to avoid these problems.

4.1. Heat Transfer

For isothermality in the packed bed reactor, the problem of temperature gradients in local areas of the reactor can be significantly improved by using the differential form of packed bed reactor instead of integral operation. The thin catalyst bed can allow assuming a constant of temperature, pressure, and concentration across the catalyst bed [102]. However, the problem of the differential packed bed reactor is the analysis of the product composition due to small incremental conversion. It is hard to measure the composition in a complex multicomponent system. On the other hand, the integral packed bed reactor should be ensured that exothermicity and endothermicity of reactions cannot affect the temperature profile along the catalyst bed. Besides, the dilution of feed and catalyst and reducing reactor diameter can improve temperature gradient inside packed bed reactor [13]. Carefully, decreasing reactor diameter should

be accompanied by reducing particle diameter to provide the plug-flow condition. Nevertheless, the pressure drop can appear inside the reactor if the particle diameter is very small. In other words, this problem can be eliminated by using catalyst mixed with inert particles with a suitable size to achieve a good heat distribution and a low-pressure drop.

For heat transfer in gradient-less recycle reactor, isothermal conditions are achieved more easily than in the packed bed reactor due to low conversion over the catalyst bed [1]. The turbulence inside the CSTR type reactor affects excellent heat transfer, especially for LS (liquid-solid) reaction systems. The catalyst can be suspended in the fluid. However, the temperature profile in some types of gradient-less recycle reactors cannot be measured inside the reactor. The reactors operated with spinning catalyst baskets such as the Carberry reactor or Robinson-Mahoney spinning catalyst basket reactor are inapplicable to measure the temperature due to the movement of the catalyst bed. Thus, highly- exothermic or endothermic reactions should be avoided for use in these reactors.

To verify a good heat transfer, the thermocouple should be installed to measure temperature at catalyst bed for both cases of packed bed reactor and gradient-less recycle reactor. Although the temperature profile along the whole length of the packed bed reactor is usually non-isothermal, the temperature along the catalyst bed should be in the isothermal zone at the desired temperature to avoid heat transfer limitation. For the reactors, which the temperature profile cannot be measured, such as Carberry reactor, Mear's criterion and the parameter group of Carberry number (Ca), Prater number (β_{ex}), and dimensionless activation energy (γ^E) can be used to investigate the limitation of extra-particle heat transfer, as shown in Table 4. Carberry number (Ca) represents the concentration profile over the resistance film. The Prater number (β_{ex}) can determine the maximum temperature drop or rise due to endothermic or exothermic reaction, whereas the dimensionless activation energy (γ^E) determines the sensitivity of the reaction towards a temperature change. If this group is much less than 0.05, the limitation of extra-particle heat transfer can be ignored. As same as Mear's criterion, the value should be lower than 0.15.

For intra-particle heat transfer, the group of Prater number (β_{ex}), dimensionless activation energy (γ_s^E), and Wheeler-Weisz parameter ($\eta_{in}\phi^2$) is used to determine this limitation, as shown in Eq. (45) (Table 4). The Wheeler-Weisz parameter represents the concentration profile inside porous catalyst, whereas dimensionless activation energy (γ_s^E) is considered at the particle surface. Unfortunately, the concentration and the temperature at the catalyst surface (C_s and T_s) are not always known. Thus, using these values of bulk-phase is acceptable. If this group of three parameters is much lower than 0.05, the intra-particle heat transfer is effective.

4.2. External Diffusion

For external mass diffusion in the packed bed reactor, it is well-known that there is resistance film between catalyst particle and bulk fluid in gas-solid (GS) or liquid-solid (LS) reaction system. This resistance affects the extent of concentration gradient; moreover, it results in the error in intrinsic kinetic modeling when considering kinetic experiments with these limitations. In general, the increasing flow rate can improve the external mass transfer and suppress resistance films. It reduces the concentration gradient between bulk fluid and external catalyst surface due to a thinner resistance film. According to Perego and Peratello (1999), the flow rate test, as shown in Fig. 20, can be used to test the limitation of external diffusion for the packed bed reactor [13]. The set of experiments is carried out by increasing both feed flow rate (F) and the amount of catalyst (V), whereas the space velocity (GHSV or LHSV) is kept as a constant. The conversion will change until there is no limitation of external mass diffusion. According to Sripinun et al. (2015) and Kasempremchit et al. (2016), they used this set of experiments for investigating the external diffusion to avoid this limitation in their kinetic measurement [103, 104].

For external mass transfer in gradient-less recycle reactor, increasing fluid velocity inside the reactor can also improve the external mass transfer as same as the packed bed reactor. The simple experimental method for determining external mass diffusion inside the gradient-less recycle reactor is increasing impeller speed with the same amount of catalyst (V), as shown in Fig. 21. If the impeller speed is high enough, the limitation of external mass transfer can be neglected. According to Ountaksinkul et al. (2020), this set of experiments was applied with the gradient-less Berty reactor for 1-butene isomerization over MgO catalyst [49]. It was found that the limitation of external mass transfer can be observed at relatively low impeller speed. At the same time, the 1-butene conversion was not changed at impeller speed above 1500 rpm or with no limitation of external mass diffusion. Besides the experimental methods, the limitation of external mass transfer can be additionally determined by the theoretical criteria, as shown in Eq. (39) and (40) (Table 4). The Carberry number and Mear's criterion can be used to consider these limitations. The observed rate of reaction, bulk concentration, mass transfer coefficient, and particle size are used to calculate both criteria based on experimental observation. If the Carberry number is lower than 0.05, the effect of the external mass transfer can be neglected. Whereas Mear's criterion should be less than 0.15.
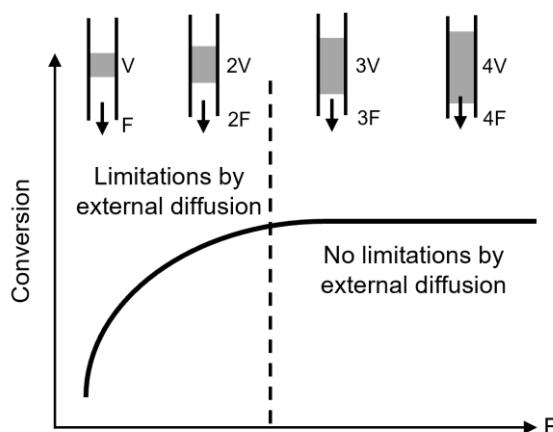

Fig. 20. Experimental test for evaluating the external diffusion in packed bed reactor (Adapted from [13]).
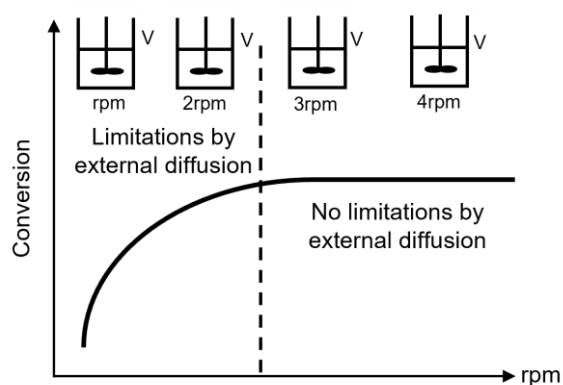

Fig. 21. Experimental test for evaluating the external diffusion in gradient-less recycle reactor.

4.3 Internal Diffusion

For internal mass transfer in the packed bed reactor, the simplest method to avoid the limitation of pore diffusion is a reduction of particle diameter as far as possible. However, as mentioned above, the pressure drop problem can arise when the particle diameter is too small. Figure 22 shows the experimental test for evaluating the internal diffusion in the packed bed reactor. The set of experiments are carried out by reducing particle diameter (d_p), whereas the amount of catalyst (V) and flow rate (F) are kept as a constant [13]. The space velocity was fixed in all experiments under identical conditions. Variation of the particle diameter can be provided by crushing and sieving the catalyst. If the conversion is changed by decreasing particle diameter, it can be considered that the reaction rate is limited by internal mass diffusion. On the other hand, a steady conversion can refer to the system under chemical kinetics control at small particle size. Cautiously, the limitation of external mass transfer can stimulate particle size dependence. The effect of flow should not be included in this experimental diagnostic test; furthermore, heat transfer should also be avoided.

Table 4. Criteria for determining transport limitations for a catalyst particle under steady state condition.

| Transport process	Criterion	Eqs.	Ref.
External mass transfer			
Carberry number	$Ca = \dfrac{r_{obs}}{k_g a' C_b} < 0.05$	(39)	[3]
Mear's criterion	$\dfrac{-r'_{obs}\rho_b R n}{k_g C_b} < 0.15$	(40)	[93]
Internal mass transfer			
Weisz-Prater criterion	$C_{WP} = \dfrac{(-r'_{obs})\rho_c R^2}{D_e C_s} < 1$	(41)	[93]
Wheeler-Weisz criterion	$\eta_{in}\phi^2 = \dfrac{r_{obs}L^2}{D_e C_s}\left(\dfrac{n+1}{2}\right) < 0.1$	(42)	[3]
Weisz & Hicks criterion	$\dfrac{r_{obs}\rho_c R^2}{C_b D_e}\left[exp\left(\dfrac{\gamma\beta_T}{1+\beta_T}\right)\right] < 1$	(1)	[105]
Extra-particle heat transfer			
Carberry number	$\|\beta_{ex}\gamma^E Ca\| = \left\|\dfrac{k_g(-\Delta H)C_b}{hT_b}\right\|\dfrac{E_a}{R_G T_b}Ca < 0.05$	(43)	[3]
Mear's criterion	$\left\|\dfrac{-\Delta H(-r'_{obs})\rho_b R E_a}{hT^2 R_G}\right\| < 0.15$	(44)	[93]
Intra-particle heat transfer			
	$\|\beta_{in}\gamma_s^E(\eta_{in}\phi^2)\| = \left\|\dfrac{D_e(-\Delta H)C_s}{\lambda_e T_s}\right\|\dfrac{E_a}{R_G T_s}(\eta_{in}\phi^2) < 0.05$	(45)	[3]
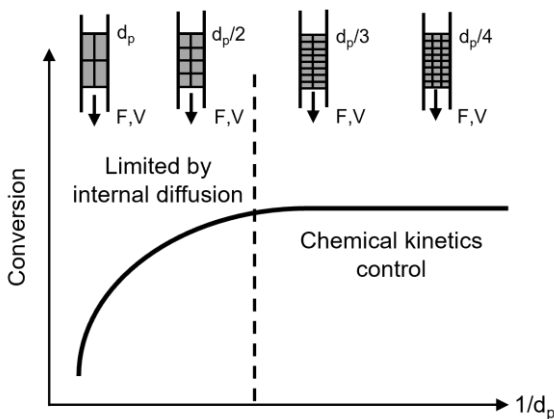
Fig. 22. Experimental test for evaluating the internal diffusion in packed bed reactor (Adapted from [13]).

Unfortunately, this simple method cannot be applied with the gradient-less recycle reactor. To achieve perfect mixing in the gradient-less recycle reactor, the recirculation inside the reactor is extremely high. The catalyst loss out of the reactor and the accumulation at the exit can occur when the catalyst is very small. Therefore, theoretical criteria are used to determine the internal mass diffusion in the gradient-less recycle reactor. As shown in Table 4 (Eqs. (1), (41), and (42)), the criteria of Weisz-Prater, Wheeler-Weisz, and Weisz-Hicks can be used to verify the absence of pore diffusion. Theoretically, the Weisz-Prater criterion was defined with the assumptions of steady-state condition, the spherical shape of catalyst pellet, and diffusion occurred in radial direction only. The rate of reaction, the solid density of the catalyst, the effective diffusion coefficient, and particle size can be obtained from experimental observation as well. Whereas

the concentration at the catalyst surface (C_s) cannot be measured in the real experiment. Consequently, it can be assumed to be equal to the bulk concentration (C_b). If $\eta_{in}\phi^2$ is much less than 0.1 for the Wheeler-Weisz criterion, the limitation of internal mass transfer can be neglected. While the other criteria should be lower than 1.

5. Conclusion & Perspectives

In order to study intrinsic kinetics, the two common laboratory reactors, i.e., packed bed reactor and gradient-less recycle reactor, have been employed over the last century. The main advantages of these reactors are an uncomplicated system, and low investment and operating costs compared with others [106]. Generally, a small amount of catalyst is loaded in the laboratory reactor in the range from 0.01 to 1 g, and gas flow rates are usually between 10 and 1000 cm³ min⁻¹ (STP) [1]. The gradient-less recycle reactor typically requires more catalyst and a higher flow rate. Due to the larger volume, it takes a longer time for the gradient-less-recycle reactor to reach steady state of chemical reactions taking place in the reactor. Therefore, this reactor cannot immediately determine the conversion or deactivation. Moreover, the catalyst bed temperature in some types of gradient-less recycle reactor (such as the Carberry reactor and Robinson-Mahoney spinning catalyst basket reactor) cannot be measured owing to the rotation of the catalyst bed. Consequently, the highly exothermic or endothermic reactions should be avoided in these reactors. The problem of internal mass diffusion should also be concerned in this reactor because of the use of large catalyst particles to avoid the pressure drop problem across the catalyst bed while obtaining high

recirculation rates [1]. On the other hand, when the particle size is too small, the catalyst can lose out of the reactor or accumulate at the exit. Regarding flow characteristics, several research papers confirmed that non-ideal flow characteristics (e.g., dead zone, bypassing) still exits under some operating conditions for the original Berty-type reactor, especially at atmospheric pressure [9, 68]. Due to this limitation, selection of suitable operating conditions to obtain intrinsic kinetic data is important.

However, the gradient-less recycle reactor has been continuously developed to solve this problem. The latest design of the ILS-Berty internal recycle reactor can overcome the use of this reactor at atmospheric pressure with the perfect mixing regime. This reactor was established by Integrated Lab Solutions (ILS) and Friedrich-Alexander University, Erlangen, Germany [79]. Due to compact design and extremely high impeller speeds, the ILS Berty reactor can be used to investigate intrinsic catalyst properties without all transport limitations and provide the perfect mixing region under testing conditions at high temperatures up to 600 °C and atmospheric pressure or nearby. Moreover, the gradient-less recycle reactor can be generally used under industrial conditions over commercial catalysts. An algebraic equation of the ideal CSTR model, which is the simplest method, can be applied for intrinsic kinetic modeling and the reaction rate can be directly estimated from conversions.

For the packed bed reactor, a smaller amount of catalyst and lower flow rate are provided when compared with the gradient-less recycle reactor, especially in differential fixed bed reactor. Due to the relatively low conversion of the differential packed reactor, the problem of the non-isothermal condition can be easily solved. In contrast, a highly exothermic or endothermic reaction should be avoided for the integral packed bed reactor. Besides, the limitations of external and internal mass transfers can be investigated by the experimental diagnostic tests as mentioned in the section 4. To avoid the limitations of mass transfers, particle size is usually reduced; furthermore, the small particle size of the catalyst particle can also provide an excellent heat transfer in the packed bed reactor. However, the problem of pressure drop can appear when the particle size of the catalyst is too small. Therefore, using a catalyst with the proper particle size can eliminate these limitations with a low-pressure drop. Nevertheless, the crushing of the catalyst particles is not always conclusive. The other shapes, such as eggshells, zeolites, and wash-coated monoliths, can also be used for catalyst testing. For example, the layer thickness of wash-coated monoliths can generally give the particle size smaller than 50 μm, which the crushing catalyst cannot provide. For plug flow operation, some conditions can be fulfilled to verify the plug flow pattern as described in the section 2.1. The ordinary differential equation (ODE) of the plug flow model can be generally used for intrinsic kinetic modeling when the absence of transport limitations and plug flow pattern are ensured. In some cases, the non-ideal flow characteristics of mixing

dispersion can occur in the packed bed reactor. The axial dispersion (ADM) model is an alternative method for applying intrinsic kinetic modeling to extract this problem. In addition, more detailed discussions of laboratory reactors can be found elsewhere [1, 2, 107-109].

The intrinsic catalyst properties (intrinsic activity, selectivity, and deactivation) during the kinetic experiments are achieved by applying the following conditions:

- Ideal flow behaviors (plug flow for PFR or perfect mixing for CSTR) should be verified to interpret kinetic data directly.
- Internal and external mass transfer limitations, as well as heat transfer limitations, should be avoided to determine intrinsic kinetic data.
- It should be ensured that the catalytic activity is obtained at the steady-state condition.
- In case of the system having unavoidable transport limitations or catalyst deactivation, these effects should be taken into account in the mathematical model.

Although both packed bed reactor and gradient-less recycle reactor are possible to determine intrinsic kinetics effectively, some valuable information for sequences of reaction network should be considered to provide intrinsic kinetic parameters suitably. It is difficult to obtain this information from both packed bed reactor and gradient-less recycle reactor. Therefore, the modern technologies for transient laboratory reactors, such as the steady-state isotopic transient kinetic analysis (SSITKA) or the temporal analysis of products (TAP) reactor, are the essential tools to study the reaction mechanisms of various chemical reactions. In conclusion, the selection of suitable laboratory reactors for determining intrinsic kinetics depends on several factors: the reaction system (GS or LS system, etc.), transport limitations, flow characteristics in studied operating conditions, suitable contact between reactant and catalyst, and interpretation of kinetic data. There is no best laboratory reactor for all types of reactions and catalysts.

For the current trend, the high throughput microreactor (HTMR) has the potential to determine intrinsic kinetics due to the two major advantages. First, the compact system of HTMR can provide excellent heat- and mass- transfers. Consequently, kinetic data obtained from HTMR are free from limitations of external and internal mass transfers as well as heat transfer. Moreover, catalyst coating in the wall of HTMR can reduce pressure drop, which is one of the factors affecting kinetic modeling. Second, HTMR can also test catalysts in parallel operation with the different operating conditions. This HTMR is more convenient for collecting kinetic data than the conventional single bed reactors (fixed bed reactor and gradient-less recycle reactor). In addition, a new challenge for high-throughput experimentation is a design together with machine learning to broaden the boundaries of practical applications. According to Kumar et al. (2019), the strategy, which machine learning, data management,

high-throughput experimentation, and simulations could be combined together to create a system for predicting polymer properties, was discussed [110]. It enables researchers to generate the system for designing products based on desired properties. The similar concept could be extended for determining intrinsic kinetics.

Nomenclature

a', a_c	specific surface area of particle (m² m⁻³)
A_0	pre-exponential factor
B	constant characterizing the gradient-less reactor
Ca	Carberry number
C_i, C_A	concentration of species i or A (mol m⁻³)
C_b	concentration at bulk-phase (mol m⁻³)
C_s, C_{As}	concentration at external catalyst surface (mol m⁻³)
$C_{p,i}$	concentration within catalyst pellet of species i (mol m⁻³)
C_T	exit concentration (mol m⁻³)
C_{Ts}	concentration of non-stationary volume (mol m⁻³)
C_{T0}	initial or total concentration (mol m⁻³)
d, d_p	particle diameter (m)
D	inner diameter of reactor (m)
D_A, D_m	molecular diffusion coefficient (m² s⁻¹)
D_{ax}	axial dispersion coefficient (m² s⁻¹)
D_e	effective diffusion coefficient (m² s⁻¹)
E_a	activation energy (kJ kmol⁻¹)
$E(t)$	exit age distribution curve
F_{i0}	inlet mole flow rate of species i (mol s⁻¹)
F_i, F_A	outlet mole flow rate of species i or A (mol s⁻¹)
h	heat transfer coefficient between bulk gas and pellet (kJ m⁻² s⁻¹ K⁻¹)
ΔH	heat of reaction or heat enthalpy (kJ mol⁻¹)
k	kinetic constant
k_r	intrinsic kinetic constant
k_{app}	apparent kinetic constant
k_b	kinetic constant for backward reaction
k_f	kinetic constant for forward reaction
k_g, k_c	mass transfer coefficient (m s⁻¹)
K_{eq}	equilibrium constant
L	characteristic length or bed length (m)
p	partial pressure (atm)
ΔP	pressure drop (atm)
Pe	Péclet number
Pe_p	Péclet number based on particle properties
n	reaction order
N_i	mole of species i (mol)
Q_b	bypassing volumetric flow rate (m³ s⁻¹)
Q_t	non-bypassing volumetric flow rate (m³ s⁻¹)
Q_0	total volumetric flow rate (m³ s⁻¹)
r	distance in radius of catalyst pellet (m)

r_i, r_A	volumetric reaction rate of species i or A (mol m⁻³ s⁻¹)
r_i', r_A'	reaction rate by catalyst weight of species i or A (mol g-cat⁻³ s⁻¹)
$r_{i,p}$	reaction rate of the component i in reaction step p (mol g-cat⁻³ s⁻¹)
r_{obs}	observed volumetric reaction rate (mol m⁻³ s⁻¹)
r_{obs}'	observed reaction rate by catalyst weight (mol g-cat⁻³ s⁻¹)
R, R_p	catalyst particle radius (m)
R_G	gas constant (J mol⁻¹ K⁻¹)
Re	Reynolds number
S_i	source term of species i in axial dispersion model (mol m⁻² s⁻¹)
Sc	Schmidt number
Sh	Sherwood number
t	time (s)
$\bar{t}$	average residence time (s)
T, T_b	bulk temperature (°C or K)
T_s	temperature at particle surface (°C or K)
u_0, u_s	superficial velocity of fluid (m s⁻¹)
v	interstitial velocity (m s⁻¹)
V	total reactor volume (m³)
V_t	non-stationary volume (m³)
V_d	dead volume (m³)
w	rotation speed (rev/s)
W	catalyst weight (g)
z	distance in the reactor (m)

Greek Symbols

α	fraction of non-stationary volume to total volume
β	fraction of bypassing to total volumetric flow rate
β_T	maximum temperature variation within particle relative to the boundary temperature
β_{ex}	external Prater number
ε	effective porosity of the reactor bed $[= \varepsilon_b + (1 - \varepsilon_b)\varepsilon_p]$
ε_b	void fraction of reactor
ε_p	particle porosity
η_{in}	internal effectiveness factor
ϕ	Thiele modulus
ρ	fluid density (kg m⁻³)
ρ_b	bulk density of catalyst bed (kg m⁻³)
ρ_c	solid density of catalyst (kg m⁻³)
τ	mean residence time (s)
μ	fluid viscosity (Pa s)
v	interstitial velocity (m s⁻¹)
$v_{i,p}$	stoichiometric number of the component i in reaction step p
γ^E	dimensionless activation energy at bulk-phase
γ, γ_s^E	dimensionless activation energy at particle surface

λ_e effective thermal conductivity (W m^{-1} K^{-1})

Abbreviations

CSTR   continuous stirred-tank reactor
CFD   computational fluid dynamics
LHHW   Langmuir-Hinshelwood-Hougen-Watson
ODE   ordinary differential equation
PDE   partial differential equation
PFR   plug-flow reactor
RTD   residence time distribution
SSITKA   steady-state isotopic transient kinetic analysis
TAP   temporal analysis of product reactor
HTE   high throughput experimentation
HTMR   high throughput microreactor

Acknowledgement

References

[1] F. Kapteijn and J. A. Moulijn, "Laboratory testing of solid catalysts," in *Handbook of Heterogeneous Catalysis*. Wiley, 2008, pp. 2019-2045.

[2] R. J. Berger, E. H. Stitt, G. B. Marin, F. Kapteijn, and J. A. Moulijn, "Eurokin. Chemical reaction kinetics in practice," *Cattech*, vol. 5, no. 1, pp. 36-60, 2001, doi: 10.1023/a:1011928218694.

[3] R. J. Berger *et al.*, "Dynamic methods for catalytic kinetics," *Applied Catalysis A: General,* vol. 342, no. 1-2, pp. 3-28, 2008, doi: 10.1016/j.apcata.2008.03.020.

[4] G. Ertl, H. Knozinger, and J. Weitkamc, "Kinetics and Transport Processes," in *Handbook of Heterogeneous Catalysis*. Wiley, 1997, ch. 6, pp. 1190-1260.

[5] J. Van Belleghem, D. Constales, J. W. Thybaut, and G. B. Marin, "Complex reaction network generation for steady state isotopic transient kinetic analysis: Fischer-Tropsch Synthesis," *Computers & Chemical Engineering,* vol. 125, pp. 594-605, 2019, doi: 10.1016/j.compchemeng.2016.07.003.

[6] G. Creten, D. S. Lafyatis, and G. F. Froment, "Transient kinetics from the tap reactor system: Application to the oxidation of propylene to acrolein," *Journal of Catalysis,* vol. 154, no. 1, pp. 151-162, 1995. [Online]. Available: https://doi.org/10.1006/jcat.1995.1156.

[7] G. S. Yablonsky, D. Constales, S. O. Shekhtman, and J. T. Gleaves, "The Y-procedure: How to extract the chemical transformation rate from reaction–diffusion data with no assumption on the kinetic model," *Chemical Engineering Science,* vol. 62, no. 23, pp. 6754-6767, 2007, doi: 10.1016/j.ces.2007.04.050.

[8] L. Lukashuk and K. Föttinger, "In situ and operando spectroscopy: A powerful approach towards understanding of catalysts," *Johnson Matthey Technology Review,* vol. 62, 2018, doi: 10.1595/205651318X15234323420569.

[9] H. Hannounf and J. R. Regalbuto, "Mixing characteristics of a micro-berty catalytic reactor," *Industrial & Engineering Chemistry Research,* vol. 31, pp. 1288-1292, 1992, doi: 10.1021/ie00005a008.

[10] P. Toson, P. Doshi, and D. Jajcevic, "Explicit residence time distribution of a generalised cascade of continuous stirred tank reactors for a description of short recirculation time (bypassing)," *Processes,* vol. 7, no. 9, 2019, doi: 10.3390/pr7090615.

[11] M. Mohagheghi, G. Bakeri, and M. Saeedizad, "Study of the effects of external and internal diffusion on the propane dehydrogenation reaction over Pt-Sn/Al$_2$O$_3$ catalyst," *Chemical Engineering & Technology,* vol. 30, no. 12, pp. 1721-1725, 2007, doi: 10.1002/ceat.200700157.

[12] R. I. Masel, *Principles of Adsorption and Reaction on Solid Surfaces*, 1st ed. United States of America: A Wiley-Interscience publication, 1951.

[13] C. Perego and S. Peratello, "Experimental methods in catalytic kinetics," *Catalysis Today,* vol. 52, no. 2, pp. 133-145, 1999. [Online]. Available: https://doi.org/10.1016/S0920-5861(99)00071-1.

[14] N. Y. Chen, T. F. Degnan Jr., and C. M. Smith, *Molecular Transport and Reaction in Zeolites: Design and Application of Shape Selective Catalysis*. John Wiley & Sons, 1994.

[15] D. L. Cresswell, "On the uniqueness of the steady state of a catalyst pellet involving both intraphase and interphase transport," *Chemical Engineering Science,* vol. 25, no. 2, pp. 267-275, 1970. [Online]. Available: https://doi.org/10.1016/0009-2509(70)80020-3.

[16] E. L. Cussler and E. L. Cussler, *Diffusion: Mass Transfer in Fluid Systems*. Cambridge University Press, 2009.

[17] J. B. Butt, *Reaction Kinetics and Reactor Design*. CRC Press, 2000.

[18] J. M. Berty, "The recycle reactor concept," in *Experiments in Catalytic Reaction Engineering,* vol. 124, B. Delmon and J. T. Yates, Eds. 1999, ch. 3.

[19] S. O. Shekhtman, G. S. Yablonsky, S. Chen, and J. T. Gleaves, "Thin-zone TAP-reactor—Theory and application," *Chemical Engineering Science,* vol. 54, no. 20, pp. 4371-4378, 1999. [Online]. Available: https://doi.org/10.1016/S0009-2509(98)00534-X.

[20] V. Frøseth, S. Storsæter, Ø. Borg, E. A. Blekkan, M. Rønning, and A. Holmen, "Steady state isotopic transient kinetic analysis (SSITKA) of CO hydrogenation on different Co catalysts," *Applied Catalysis A: General,* vol. 289, no. 1, pp. 10-15, 2005.

[21] D. V. Kozlov, A. V. Vorontsov, P. G. Smirniotis, and E. N. Savinov, "Gas-phase photocatalytic oxidation of diethyl sulfide over TiO2: Kinetic investigations and catalyst deactivation," *Applied Catalysis B: Environmental,* vol. 42, no. 1, pp. 77-87, 2003. [Online].

Available: https://doi.org/10.1016/S0926-3373(02)00217-5.

[22] J. T. Gleaves, G. Yablonsky, X. Zheng, R. Fushimi, and P. L. Mills, "Temporal analysis of products (TAP)—Recent advances in technology for kinetic analysis of multi-component catalysts," *Journal of Molecular Catalysis A: Chemical,* vol. 315, no. 2, pp. 108-134, 2010, doi: 10.1016/j.molcata.2009.06.017.

[23] J. T. Gleaves, J. R. Ebner, and T. C. Kuechler, "Temporal Analysis of Products (TAP)—A unique catalyst evaluation system with submillisecond time resolution," *Catalysis Reviews,* vol. 30, no. 1, pp. 49-116, 1988, doi: 10.1080/01614948808078616.

[24] D. J. Statman, J. T. Gleaves, D. McNamara, P. L. Mills, G. Fornasari, and J. R. H. Ross, "TAP reactor investigation of methane coupling over samarium oxide catalysts," *Applied Catalysis,* vol. 77, no. 1, pp. 45-53, 1991. [Online]. Available: https://doi.org/10.1016/0166-9834(91)80022-O.

[25] C. Ledesma, J. Yang, D. Chen, and A. Holmen, "Recent approaches in mechanistic and kinetic studies of catalytic reactions using SSITKA technique," *ACS Catalysis,* vol. 4, no. 12, pp. 4527-4547, 2014, doi: 10.1021/cs501264f.

[26] S. H. Ali and J. G. Goodwin, "SSITKA investigation of palladium precursor and support effects on CO hydrogenation over supported Pd catalysts," *Journal of Catalysis,* vol. 176, no. 1, pp. 3-13, 1998. [Online]. Available: https://doi.org/10.1006/jcat.1998.1993.

[27] G. G. Olympiou, C. M. Kalamaras, C. D. Zeinalipour-Yazdi, and A. M. Efstathiou, "Mechanistic aspects of the water–gas shift reaction on alumina-supported noble metal catalysts: In situ DRIFTS and SSITKA-mass spectrometry studies," *Catalysis Today,* vol. 127, no. 1, pp. 304-318, 2007. [Online]. Available: https://doi.org/10.1016/j.cattod.2007.05.002.

[28] R. Meijer, F. Kapteijn, and J. A. Moulijn, "Kinetics of the alkali-carbonate catalysed gasification of carbon: 3. H$_2$O gasification," *Fuel,* vol. 73, no. 5, pp. 723-730, 1994.

[29] J. Moulijn, A. Tarfaoui, and F. Kapteijn, "General aspects of catalyst testing," *Catalysis Today,* vol. 11, no. 1, pp. 1-12, 1991.

[30] J. Ross, "Catalytic reactors and the measurement of catalytic kinetics," in *Heterogeneous Catalysis*. Elsevier, 2012, pp. 97-121.

[31] O. Levenspiel, *Chemical Reaction Engineering*, 3th ed. United States of America: John Wiley & Sons, 1999.

[32] K. Ountaksinkul *et al.*, "Performance comparison of different membrane reactors for combined methanol synthesis and biogas upgrading," *Chemical Engineering and Processing - Process Intensification,* vol. 136, pp. 191-200, 2019, doi: 10.1016/j.cep.2019.01.009.

[33] S. V. Gokhale, R. K. Tayal, V. K. Jayaraman, and B. D. Kulkarni, "Microchannel reactors: Applications and use in process development," *International Journal of Chemical Reactor Engineering,* vol. 3, no. 1, 2005.

[34] N. Engelbrecht, R. C. Everson, D. Bessarabov, and G. Kolb, "Microchannel reactor heat-exchangers: A review of design strategies for the effective thermal coupling of gas phase reactions," *Chemical Engineering Processing-Process Intensification,* vol. 157, p. 108164, 2020.

[35] A. Gavriilidis, P. Angeli, E. Cao, K. Yeong, and Y. Wan, "Technology and applications of microengineered reactors," *Chemical Engineering Research Design,* vol. 80, no. 1, pp. 3-30, 2002.

[36] N. R. Peela and D. Kunzru, "Steam reforming of ethanol in a microchannel reactor: kinetic study and reactor simulation," *Industrial Engineering Chemistry Research,* vol. 50, no. 23, pp. 12881-12894, 2011.

[37] S. Hu *et al.*, "Kinetic study of ionic liquid synthesis in a microchannel reactor," *Chemical Engineering Journal,* vol. 162, no. 1, pp. 350-354, 2010.

[38] M. Tahir and N. S. Amin, "Photocatalytic CO$_2$ reduction and kinetic study over In/TiO$_2$ nanoparticles supported microchannel monolith photoreactor," *Applied Catalysis A: General,* vol. 467, pp. 483-496, 2013.

[39] V. Paunovic, J. C. Schouten, and T. A. Nijhuis, "Direct synthesis of hydrogen peroxide using concentrated H$_2$ and O$_2$ mixtures in a wall-coated microchannel–kinetic study," *Applied Catalysis A: General,* vol. 505, pp. 249-259, 2015.

[40] C. Cao, G. Xia, J. Holladay, E. Jones, and Y. Wang, "Kinetic studies of methanol steam reforming over Pd/ZnO catalyst using a microchannel reactor," *Applied Catalysis A: General,* vol. 262, no. 1, pp. 19-29, 2004.

[41] J. G. Creer, P. Jackson, G. Pandy, G. G. Percival, and D. Seddon, "The design and construction of a multichannel microreactor for catalyst evaluation," *Applied Catalysis,* vol. 22, no. 1, pp. 85-95, 1986.

[42] P. Hazemann *et al.*, "Kinetic data acquisition in high-throughput Fischer–Tropsch experimentation," *Catalysis Science & Technology,* vol. 10, no. 21, pp. 7331-7343, 2020, doi: 10.1039/d0cy00918k.

[43] C. Ehm, A. Mingione, A. Vittoria, F. Zaccaria, R. Cipullo, and V. Busico, "High-throughput experimentation in olefin polymerization catalysis: Facing the challenges of miniaturization," *Industrial & Engineering Chemistry Research,* vol. 59, no. 31, pp. 13940-13947, 2020, doi: 10.1021/acs.iecr.0c02549.

[44] R. A. Potyrailo and E. J. Amis, *High-Throughput Analysis: a Tool for Combinatorial Materials Science*. Springer Science & Business Media, 2012.

[45] M. J. M. Mies, E. V. Rebrov, L. Deutz, C. R. Kleijn, M. H. J. M. de Croon, and J. C. Schouten, "Experimental validation of the performance of a microreactor for the high-throughput screening of catalytic coatings," *Industrial & Engineering Chemistry Research,* vol. 46, no. 12, pp. 3922-3931, 2007, doi: 10.1021/ie061081w.

[46] M. J. M. Mies, E. V. Rebrov, M. H. J. M. de Croon, and J. C. Schouten, "Design of a molybdenum high throughput microreactor for high temperature

screening of catalytic coatings," *Chemical Engineering Journal,* vol. 101, no. 1-3, pp. 225-235, 2004, doi: 10.1016/j.cej.2003.11.024.

[47] N. Steinfeldt, N. Dropka, D. Wolf, and M. Baerns, "Application of multichannel microreactors for studying heterogeneous catalysed gas phase reactions," *Chemical Engineering Research Design,* vol. 81, no. 7, pp. 735-743, 2003.

[48] P. Schmitz *et al.*, "NO oxidation over supported Pt: Impact of precursor, support, loading, and processing conditions evaluated via high throughput experimentation," *Applied Catalysis B: Environmental,* vol. 67, no. 3-4, pp. 246-256, 2006, doi: 10.1016/j.apcatb.2006.05.012.

[49] K. Ountaksinkul, S. Wannakao, P. Praserthdam, and S. Assabumrungrat, "Intrinsic kinetic study of 1-butene isomerization over magnesium oxide catalyst via a Berty stationary catalyst basket reactor," *RSC Advances,* vol. 10, no. 60, pp. 36667-36677, 2020, doi: 10.1039/d0ra05453d.

[50] R. Pretorius, J. le Roux, K. Wagener, D. van Vuuren, and P. Crouse, "Fluorination of neodymium carbonate monohydrate with anhydrous hydrogen fluoride in a Carberry spinning-basket reactor," *Reaction Chemistry & Engineering,* vol. 4, no. 8, pp. 1400-1409, 2019, doi: 10.1039/c8re00117k.

[51] J. Lauwaert, C. S. Raghuveer, and J. W. Thybaut, "A three-phase Robinson-Mahoney reactor as a tool for intrinsic kinetic measurements: Determination of gas-liquid hold up and volumetric mass transfer coefficient," *Chemical Engineering Science,* vol. 170, pp. 694-704, 2017, doi: 10.1016/j.ces.2017.02.041.

[52] Parker-Hannifin. "Berty stationary basket catalyst testing reactor." http://www.autoclaveengineers.com/products/catalytic_reactors/CR_Berty_Stationary_Basket/index.html (accessed Aug. 14, 2021).

[53] Parker-Hannifin. "Carberry spinning catalyst basket reactor." http://www.autoclaveengineers.com/products/catalytic_reactors/CR_Carberry_Spinning/index.html (accessed Aug. 14, 2021).

[54] P. Blumler, B. Blumich, R. Botto, and E. Fukushima, *Magnetic Resonance Microscopy.* WILEY-VCH, 1992.

[55] Parker-Hannifin. "Robinson-Mahoney stationary catalyst basket reactor." http://www.autoclaveengineers.com/products/catalytic_reactors/CR_Robinson_Mahoney_Stationary/index.html (accessed Aug. 14, 2021).

[56] Parker-Hannifin. "Robinson-Mahoney spinning catalyst basket reactor." http://www.autoclaveengineers.com/products/catalytic_reactors/CR_Mahoney_Robinson_Spinning/index.html (accessed Aug. 14, 2021).

[57] M. Estenfelder, H.-G. Lintz, B. Stein, and J. Gaube, "Comparison of kinetic data obtained from integral fixed bed reactor and differential recycle reactor," *Chemical Engineering Processing: Process Intensification,* vol. 37, no. 1, pp. 109-114, 1998.

[58] R. G. Szafran and A. Kmiec, "Application of CFD modelling technique in engineering calculations of three-phase flow hydrodynamics in a jet-loop reactor," *International Journal of Chemical Reactor Engineering,* vol. 2, no. 1, 2004.

[59] G. M. Amaral and R. Giudici, "Kinetics and modeling of fatty alcohol ethoxylation in an industrial spray loop reactor," *Chemical Engineering Technology,* vol. 34, no. 10, pp. 1635-1644, 2011.

[60] C. Ortega, M. Rezaei, V. Hessel, and G. Kolb, "Methanol to dimethyl ether conversion over a ZSM-5 catalyst: Intrinsic kinetic study on an external recycle reactor," *Chemical Engineering Journal,* vol. 347, pp. 741-753, 2018, doi: 10.1016/j.cej.2018.04.160.

[61] M. A. Al-Saleh, M. S. Al-Ahmadi, and M. A. Shalabi, "Kinetic study of ethylene oxidation in a Berty reactor," *The Chemical Engineering Journal,* vol. 37, pp. 35-41, 1988.

[62] A. N. R. Bos, E. S. Bootsma, F. Foeth, H. W. J. Sleyster, and K. R. Westerterp, "A kinetic study of the hydrogenation of ethyne and ethene on a commercial Pd/Al_2O_3 catalyst," *Chemical Engineering and Processing,* vol. 32, pp. 53-63, 1993.

[63] C. S. Raghuveer, J. W. Thybaut, and G. B. Marin, "Pyridine hydrodenitrogenation kinetics over a sulphided $NiMo/\gamma$-Al2O3 catalyst," *Fuel,* vol. 171, pp. 253-262, 2016, doi: 10.1016/j.fuel.2015.12.042.

[64] H. Schoenfelder, J. Hinderer, J. Werther, and F. J. Keil, "Methanol to olefins-prediction of the performance of a circulating fluidized-bed reactor on the basis of kinetic experiments in a fixed-bed reactor," *Chemical Engineering Science,* vol. 49, pp. 5377-5390, 1994.

[65] P. J. Jodłowski, R. J. Jędrzejczyk, A. Gancarczyk, J. Łojewska, and A. Kolodziej, "New method of determination of intrinsic kinetic and mass transport parameters from typical catalyst activity tests: Problem of mass transfer resistance and diffusional limitation of reaction rate," *Chemical Engineering Science,* vol. 162, pp. 322-331, 2017, doi: 10.1016/j.ces.2017.01.024.

[66] G. S. Yablonsky, M. Olea, and G. B. Marin, "Temporal analysis of products: basic principles, applications, and theory," *Journal of Catalysis,* vol. 216, no. 1-2, pp. 120-134, 2003, doi: 10.1016/s0021-9517(02)00109-4.

[67] V. R. Choudhary and L. K. Doraiswamy, "A Kinetic model for the isomerization of n-butene to isobutene," *Industrial & Engineering Chemistry Process Design and Development,* vol. 14, no. 3, pp. 227-235, 1975, doi: 10.1021/i260055a006.

[68] A. G. Zwahlen and J. B. Agnew, "Isobutane dehydrogenation kinetics determination in a modified Berty gradientless reactor," *Industrial & Engineering Chemistry Research,* vol. 31, no. 9, pp. 2088-2093, 1992, doi: 10.1021/ie00009a004.

[69] V. G. Gomes and O. M. Fuller, "Dynamics of propene metathesis: Physisorption and diffusion in

heterogeneous catalysis," *AIChE Journal,* vol. 42, no. 1, pp. 204-213, 1996, doi: 10.1002/aic.690420117.

[70] F. G. Botes, "The effect of a higher operating temperature on the Fischer–Tropsch/HZSM-5 bifunctional process," *Applied Catalysis A: General,* vol. 284, no. 1-2, pp. 21-29, 2005, doi: 10.1016/j.apcata.2005.01.012.

[71] P. Azadi, G. Brownbridge, I. Kemp, S. Mosbach, J. S. Dennis, and M. Kraft, "Microkinetic modeling of the Fischer-Tropsch synthesis over cobalt catalysts," *ChemCatChem,* vol. 7, no. 1, pp. 137-143, 2015, doi: 10.1002/cctc.201402662.

[72] S. G. Poulopoulos, "Catalytic oxidation of ethanol in the gas phase over Pt/Rh and Pd catalysts: kinetic study in a spinning-basket flow reactor," *Reaction Kinetics, Mechanisms and Catalysis,* vol. 117, no. 2, pp. 487-501, 2015, doi: 10.1007/s11144-015-0954-9.

[73] E. L. Fornero, D. L. Chiavassa, A. L. Bonivardi, and M. A. Baltanás, "Transient analysis of the reverse water gas shift reaction on Cu/ZrO_2 and Ga_2O_3 $/Cu/ZrO_2$ catalysts," *Journal of CO_2 Utilization,* vol. 22, pp. 289-298, 2017, doi: 10.1016/j.jcou.2017.06.002.

[74] P. Suresh Kumar, L. Korving, K. J. Keesman, M. C. M. van Loosdrecht, and G.-J. Witkamp, "Effect of pore size distribution and particle size of porous metal oxides on phosphate adsorption capacity and kinetics," *Chemical Engineering Journal,* vol. 358, pp. 160-169, 2019. [Online]. Available: https://doi.org/10.1016/j.cej.2018.09.202.

[75] J. M. Berty, "Testing commercial catalysts in recycle reactors," *Catalysis Reviews,* vol. 20, no. 1, pp. 75-96, 1979, doi: 10.1080/03602457908065106.

[76] F. Warnecke, L. Lin, S. Haag, and H. Freund, "Identification of reaction pathways and kinetic modeling of olefin interconversion over an H-ZSM-5 catalyst," *Industrial & Engineering Chemistry Research,* vol. 59, no. 28, pp. 12696-12709, 2020, doi: 10.1021/acs.iecr.0c01747.

[77] R. Brosius and J. C. Q. Fletcher, "Direct measurement of recycle ratios in internal recycle laboratory reactors," *Chemical Engineering Journal,* vol. 161, no. 1-2, pp. 196-203, 2010, doi: 10.1016/j.cej.2010.04.014.

[78] K. Ountaksinkul *et al.,* "Characterization of single-phase flow hydrodynamics in a Berty reactor using computational fluid dynamics (CFD)," *Reaction Chemistry & Engineering,* vol. 7, no. 2, pp. 361-375, 2022, doi: 10.1039/D1RE00390A.

[79] Friedrich-Alexander-University-Erlangen-Nuernberg-(FAU), "Berty reactor," German Patent DE202014006675U1, 2014.

[80] A. Nagy and T. Turek, "Novel heterogeneous reactor designs exhibiting optimal flow hydrodynamics for lab-scale gas-phase kinetic testing of full catalyst particles," in *2019 North American Catalysis Society Meeting (NAM),* 2019.

[81] C. Bäumler, Z. Urban, and M. Matzopoulos, "Enhanced methods optimize ownership costs for

catalysts," *Hydrocarbon Processing,* vol. 86, no. 6, pp. 71-78, 2007.

[82] A. N. R. Bos, L. Lefferts, G. B. Marin, and M. H. G.M. Steijns, "Kinetic research on heterogeneously catalysed processes: A questionnaire on the state-of-the-art in industry," *Appl. Catal. A: General* vol. 160, pp. 185-190, 1997.

[83] S. Wedel and J. Villadsen, "Falsification of kinetic parameters by incorrect treatment of recirculation reactor data," *Chemical Engineering Science,* vol. 38, no. 8, pp. 1346-1349, 1983.

[84] J. A. Conesa, "CSTR with dead volume and short circuit," in *Chemical Reactor Design: Mathematical Modeling and Applications.* Wiley-VCH Verlag GmgH & Co. KGaA., 2020, ch. 1.4.2.2, pp. 23-33.

[85] M. Jafari and J. S. Soltan Mohammadzadeh, "Mixing time, homogenization energy and residence time distribution in a gas-induced contactor," *Chemical Engineering Research and Design,* vol. 83, no. 5, pp. 452-459, 2005, doi: 10.1205/cherd.04207.

[86] T. Hobler, "Flow through a packed bed," in *Mass Transfer and Absorbers.* Warsaw: Wydawnictwa Naukowo-Techniczne, 1962, ch. 2.b, pp. 105-123.

[87] V. Alopaeus and H. Norden, "A calculation method for multicomponent mass transfer coefficient correlations," *Computers Chemical Engineering,* vol. 23, no. 9, pp. 1177-1182, 1999.

[88] R. W. Breault, "A review of gas-solid dispersion and mass transfer coefficient correlations in circulating fluidized beds," *Powder Technology,* vol. 163, no. 1-2, pp. 9-17, 2006.

[89] H. Ohashi, T. Sugawara, K.-I. Kikuchi, and H. Konno, "Correlation of liquid-side mass transfer coefficient for single particles and fixed beds," *Journal of Chemical Engineering of Japan,* vol. 14, no. 6, pp. 433-438, 1981.

[90] I. Macdonald, M. El-Sayed, K. Mow, and F. Dullien, "Flow through porous media-the Ergun equation revisited," *Industrial Engineering Chemistry Fundamentals,* vol. 18, no. 3, pp. 199-208, 1979.

[91] M. Kangas, T. Salmi, and D. Y. Murzin, "Skeletal isomerization of butene in fixed beds. Part 2. Kinetic and flow modeling," *Industrial & Engineering Chemistry Research,* vol. 47, no. 15, pp. 5413-5426, 2008, doi: 10.1021/ie800062m.

[92] J. Villegas, M. Kangas, R. Byggningsbacka, N. Kumar, T. Salmi, and D. Murzin, "Skeletal isomerization of 1-butene: A thorough kinetic study over ZSM-22," *Catalysis Today - CATAL TODAY,* vol. 133, pp. 762-769, 2008, doi: 10.1016/j.cattod.2007.11.022.

[93] H. S. Fogler and M. Gürmen, *Elements of Chemical Reaction Engineering.* Prentice-Hall, 1999, pp. 741-760.

[94] S. O. Rastegar and T. Gu, "Empirical correlations for axial dispersion coefficient and Peclet number in fixed-bed columns," *J Chromatogr A,* vol. 1490, pp. 133-137, Mar 24 2017, doi: 10.1016/j.chroma.2017.02.026.

[95] J. Hiby, "Longitudinal and transverse mixing during single-phase flow through granular beds," in *Interaction Between Fluids & Particles*. 1962, pp. 312-325.

[96] S. Chung and C. Y. Wen, "Longitudinal dispersion of liquid flowing through fixed and fluidized beds," *AIChE Journal,* vol. 14, no. 6, pp. 857-866, 1968.

[97] C. De Ligny, "Coupling between diffusion and convection in radial dispersion of matter by fluid flow through packed beds," *Chemical Engineering Science,* vol. 25, no. 7, pp. 1177-1181, 1970.

[98] N. W. Han, J. Bhakta, and R. Carbonell, "Longitudinal and lateral dispersion in packed beds: Effect of column length and particle size distribution," *AIChE Journal,* vol. 31, no. 2, pp. 277-288, 1985.

[99] A. M. Athalye, S. J. Gibbs, and E. N. Lightfoot, "Predictability of chromatographic protein separations: study of size-exclusion media with narrow particle size distributions," *Journal of Chromatography A,* vol. 589, no. 1-2, pp. 71-85, 1992.

[100] S. Sripinun *et al.*, "Design of hybrid pellet catalysts of WO₃/Si-Al and PtIn/hydrotalcite via dehydrogenation and metathesis reactions for production of olefins from propane," *Chemical Engineering Science,* vol. 229, 2021, doi: 10.1016/j.ces.2020.116025.

[101] S. M. Baek, J. H. Kang, K.-J. Lee, and J. H. Nam, "A numerical study of the effectiveness factors of nickel catalyst pellets used in steam methane reforming for residential fuel cell applications," *International Journal of Hydrogen Energy,* vol. 39, no. 17, pp. 9180-9192, 2014, doi: https://doi.org/10.1016/j.ijhydene.2014.04.067.

[102] J. J. Spivey, "Complete catalytic oxidation of volatile organics," *Industrial Engineering Chemistry Research,* vol. 26, no. 11, pp. 2165-2180, 1987.

[103] S. Sripinun, K. Suriye, S. Kunjara Na Ayudhyab, P. Praserthdam, and S. Assabumrungrat, "Kinetic study of 1-butene isomerization over hydrotalcite catalyst," *International Journal of Environmental and Ecological Engineering,* vol. 9, no. 5, pp. 599-602, 2015.

[104] N. Kasempremchit, P. Praserthdam, and S. Assabumrungrat, "Comparison of physically mixed and separated MgO and WO₃/SiO₂ catalyst for propylene production via 1-butene metathesis," *Korean Journal of Chemical Engineering,* vol. 33, no. 10, pp. 2842-2848, 2016, doi: 10.1007/s11814-016-0134-2.

[105] P. B. Weisz and J. S. Hicks, "The behaviour of porous catalyst particles in view of internal mass and heat diffusion effects," *Chemical Engineering Science,* vol. 17, no. 4, pp. 265-275, 1962, doi: https://doi.org/10.1016/0009-2509(62)85005-2.

[106] H. S. Fogler, "Diffusion and Reaction," in *Elements of Chemical Reaction Engineering*: Pearson Education, Inc., 2006.

[107] K. Pratt, "Small scale laboratory reactors," in *Catalysis*: Springer, 1987, pp. 173-226.

[108] J. Vern and W. Weekman, "Laboratory reactors and their limitations," *AIChE Journal,* vol. 20, no. 5, pp. 833-840, 1974.

[109] G. F. Froment and K. Waugh, *Reaction Kinetics and the Development and Operation of Catalytic Processes*. Elsevier, 2001.

[110] J. N. Kumar, Q. Li, and Y. Jun, "Challenges and opportunities of polymer design with machine learning and high throughput experimentation," *MRS Communications,* vol. 9, no. 2, pp. 537-544, 2019, doi: 10.1557/mrc.2019.54.

[111] J. Seripani, "Residence time distribution model for lab-scale reactor for propane conversion to olefins using mixed platinum tungsten catalysts," master's thesis, Chulalongkorn University, 2017.

Khunnawat Ountaksinkul, photograph and biography not available at the time of publication.

Sirada Sripinun, photograph and biography not available at the time of publication.

Panut Bumphenkiattikul, photograph and biography not available at the time of publication.

Arthit Vongachariya, photograph and biography not available at the time of publication.

Piyasan Praserthdam, photograph and biography not available at the time of publication.

Suttichai Assabumrungrat, photograph and biography not available at the time of publication.